# Multi-year observations of the tropical Atlantic atmosphere: Multidisciplinary applications of the NOAA Aerosols and Ocean Science Expeditions (AEROSE)

Nicholas R. Nalli *

*Dell Services, Federal Government, Inc.*

*NOAA/NESDIS Center for Satellite Applications and Research (STAR)*

*Camp Springs, Maryland, USA.*

Everette Joseph and Vernon R. Morris

*NOAA Center for Atmospheric Sciences, Howard University, Washington, D.C., USA.*

Christopher D. Barnet and Walter W. Wolf

*NOAA/NESDIS Center for Satellite Applications and Research (STAR), Camp Springs, Maryland, USA.*

Daniel Wolfe

*NOAA Earth System Research Laboratory (ESRL), Boulder, Colorado, USA.*

Peter J. Minnett, Malgorzata Szczodrak

and Miguel A. Izaguirre

*Rosenstiel School of Marine and Atmospheric Science, University of Miami, Miami, Florida, USA.*

Rick Lumpkin

*NOAA/OAR Atlantic Oceanographic and Meteorological Laboratory , Miami, Florida, USA.*

Hua Xie

*I.M. Systems Group, NOAA/NESDIS/STAR, Camp Springs, Maryland, USA.*

Alexander Smirnov

*Sigma Space Corporation, NASA Goddard Space Flight Center, Greenbelt, Maryland, USA.*

Jennifer Wei

*Dell Services, Federal Government, Inc. NOAA/NESDIS/STAR, Camp Springs, Maryland, USA.*

* *Corresponding author address:* N. R. Nalli, NOAA/NESDIS/STAR, Airmen Memorial Bldg Ste 204, 5211 Auth Road, Camp Springs, Maryland 20746-4304, USA.

E-mail: Nick.Nalli@noaa.gov

ABSTRACT

This paper gives an overview of a unique set of ship-based atmospheric data acquired over the tropical Atlantic Ocean during boreal spring and summer as part of ongoing National Oceanic and Atmospheric Administration (NOAA) Aerosols and Ocean Science Expedition (AEROSE) field campaigns. Following the original 2004 campaign onboard the *Ronald H. Brown*, AEROSE has operated on a yearly basis since 2006 in collaboration with the NOAA Prediction and Research Moored Array in the Tropical Atlantic (PIRATA) Northeast Extension (PNE). In this work, attention is given to atmospheric soundings of ozone, temperature, water vapor, pressure, and wind obtained from ozonesondes and radiosondes launched to coincide with low earth orbit environmental satellite overpasses (viz., MetOp and the National Aeronautics and Space Administration A-Train). Measurements such as these over the open ocean are particularly valuable because the sea surface radiative properties are well characterized, and oceans are where satellite data are expected to make a significant impact on numerical weather prediction. Furthermore, the PNE/AEROSE campaigns are unique in their range of marine meteorological phenomena germane to the satellite missions in question, including dust and smoke outflows from Africa, the Saharan air layer (SAL), the distribution of tropical water vapor and tropical Atlantic ozone. The multi-year PNE/AEROSE sounding data are therefore valuable as correlative data for empirical "proxy datasets" (i.e., sensor data approximated from existing satellite systems with similar specifications) used in pre-launch phase calibration/validation (cal/val) of the planned Joint Polar Satellite System (JPSS) and NOAA Geosynchronous Operational Environmental Satellite R-series (GOES-R) systems, as well as numerous other science applications. A brief summary of these data, along with an overview of some important science highlights, including

meteorological phenomena of general interest, are presented.

# 1. Introduction and Background

The tropical Atlantic Ocean is a region of significant meteorological and oceanographic interest in terms of atmospheric chemistry and mesoscale-to-synoptic dynamical and thermodynamical processes. Non-maritime air masses from the African continent advect out over the Atlantic within easterly winds and waves, significantly impacting the meteorology and climate dynamics downstream into the Western Hemisphere. In particular, large-scale outflows of Saharan dust extend well out over the Atlantic within persistent stable layers of dry and warm air collectively referred to as the Saharan air layer (SAL) (e.g., Carlson and Prospero 1972; Zhang and Pennington 2004; Dunion and Velden 2004; Nalli et al. 2005). Additionally, finer mode smoke aerosols from biomass burning to the south also advect over the Atlantic, which in turn has an impact the regional atmospheric chemistry.

Acquiring synoptic-scale observations over oceans using conventional *in situ* methods is a difficult and impractical task, typically leaving marine atmospheres severely undersampled, an undesirable situation given that oceans play a major role in atmospheric forcing. An obvious solution would be the use of remotely sensed data from visible, infrared (IR) and microwave (MW) sensors onboard geo- and sun-synchronous environmental satellites. However, the unusual nature of the African continental influence over the otherwise maritime environment of the Atlantic presents a challenge for satellite retrievals. Among other things, dust aerosols introduce a systematic perturbation to satellite measured IR spectral radiances (mostly through absorption and re-emission) that can negatively impact geophysical param-

eter retrievals (e.g., Stowe and Fleming 1980; Nalli and Stowe 2002; Weaver et al. 2003). To date, the impact of dust aerosols on satellite retrievals has not been fully accounted for in operational products. Furthermore, the SAL itself is defined by very sharp vertical temperature and moisture gradients that are difficult to resolve in the vertical using passive sounders (cf. Nalli et al. 2005, 2006).

*The Aerosols and Ocean Science Expeditions (AEROSE)*

To address these topics related to the measurement of African dust and smoke phenomena (e.g., as addressed by Kahn et al. 2004) over the tropical Atlantic, the U.S. National Oceanic and Atmospheric Administration (NOAA), in collaboration with the Howard University NOAA Center for Atmospheric Sciences (NCAS), has supported as series of multidisciplinary, trans-Atlantic Aerosols and Ocean Science Expeditions (AEROSE) onboard the blue-water NOAA Ship *Ronald H. Brown* (Figure 1) to acquire simultaneous *in situ* and remotely sensed marine data during intensive observing periods. Following the first AEROSE in 2004, a number of AEROSE follow-up campaigns have been conducted as a synergistic component of the NOAA Prediction and Research Moored Array in the Tropical Atlantic (PIRATA) Northeast Extension (PNE) (Bourlès et al. 2008) project. As a complement of the PNE cruises, the multi-year AEROSE program has grown to become one of the most extensive collections of *in situ* measurements over the tropical Atlantic Ocean.

The three central scientific questions addressed by AEROSE, described in Morris et al. (2006), are: (1) What is the extent of change in the dust and smoke aerosol distributions as they evolve physically and chemically during trans-Atlantic transport? (2) How do Saharan

and sub-Saharan outflows affect the regional atmosphere and ocean during trans-Atlantic transport? (3) What is the capability of satellite remote sensing and numerical models for resolving and studying the above processes? This paper summarizes the campaigns with an eye toward the third mission objective, namely calibration/validation (cal/val) of environmental satellite observing systems. In particular, we elaborate on value of the AEROSE data for demonstrating the capability of advanced satellite sounders to observe synoptic to mesoscale phenomena like those mentioned above; it is under these "hard," but meteorologically interesting, circumstances that they can potentially have the greatest positive impact for numerical weather prediction (NWP).

---

**Sidebar:** AEROSE and Educational Partnerships

The AEROSE campaigns form an essential component of the Howard University NOAA Center for Atmospheric Sciences (NCAS) research and education program. NCAS is a NOAA Cooperative Science Center funded by the NOAA Office of Education's Educational Partnership Program (Morris et al. 2007). It is one of five such Centers aligned with a NOAA line office (in this case the National Environmental Satellite Data and Information Service, the National Weather Service and the Office of Oceanic and Atmospheric Research) (for more information see Robinson et al. 2008). While the chief aim of AEROSE is to study the impacts of air mass outflows from West Africa on the atmosphere and marine boundary layer of the tropical Atlantic Ocean, we have sought an interdisciplinary approach by involving team members not only from atmospheric and oceanographic sciences but also from biology, environmental sciences, and health sciences (e.g., cultivation and genomic sequencing of fungi

and bacteria from samples). AEROSE activities have also involved coordinated activities at surface monitoring stations in Puerto Rico (Isla Magueyes at UPRM) and West Africa (at University of Dakar and in Bamako, Mali).

In addition to this, AEROSE has explicitly sought to provide unique, hands-on field experience for graduate and undergraduate students working alongside NOAA scientists and NCAS faculty aboard a state-of-the-art NOAA research vessel. Students from partnering institutions within NCAS are routine participants in the AEROSE campaigns. Students from other Cooperative Science Centers (namely CREST and ISET) have also participated on cruises. Opportunities for research are provided to advanced undergraduates who have demonstrated potential for graduate studies. To date, several graduate students from these programs have graduated or are currently working with thesis topics related to AEROSE. Many of these students are recruited from minority-serving institutions serving to increase the presence and participation of African-American, and Hispanic and Native-American students/scientists/faculty in the atmospheric and oceanic sciences (Robinson et al. 2008; Morris et al. 2010). Each AEROSE campaign offers once-in-a-lifetime opportunities by exposing these students to the various challenges of data collection, real-world problem solving, teamwork, safety, and scientific camaraderie at sea; one such experience by 2010 student M. Oyola was recently featured on *The Front Page Blog of the American Meteorological Society* (http://blog.ametsoc.org/uncategorized/not-seasick-science-smitten/).

We have specifically designed and implemented several educational activities to ensure student development and outreach during each AEROSE campaign. Specific elements include:

- *Nightly Weather Briefings.* Participating students are charged with developing and delivering weather briefings in nightly scientific meetings to assist in planning and execution of underway deployments of soundings, sampling, and other relevant measurements. [photo]

- *Scientific Seminars.* The AEROSE Science Team sponsors an evening seminar series during the cruise that features the research of participating professional scientists and faculty. These seminars are open to the entire ship and are often attended by officers and crew members. [photo]

- *Student Projects.* Each participating student is assigned a research project in support of the mission. During the mission they deploy and maintain sensors, and conduct quality control and preliminary analysis of collected data. Toward the end of each cruise, participating students are also required to give a summary on what they learned and the specific work they accomplished during the campaign. These presentations will often include basic overviews on instrumentation, data collection and research findings.

- *Shoreside Seminars.* Seminars are arranged at universities and agencies in the various ports of call when scheduling permits. For example, during a recent port of call in Barbados, one of the co-authors (V. Morris) delivered a seminar to a summer program hosted by the University of the West Indies at Cave Hill. [photo] Similar activities have been conducted with Universities and scientific researchers in Canary Islands, Argentina, Puerto Rico, Senegal, and Ghana.

- *Web Access.* AEROSE has maintained a web presence for students from high schools,

middle schools, and the community at large to post questions, follow blogs from scientists aboard the ship, and interact with the AEROSE participants. Most recently, AEROSE has exploited social networking sites by forming a group page on Facebook.

- *Scientific tours.* AEROSE scientists and students participate in ship tours arranged for local school groups and university guests.

**End of Sidebar**

*AEROSE for Satellite Sounder Cal/Val*

Of particular interest for this objective are atmospheric profile data obtained via dedicated rawinsondes and ozonesondes, described below in more detail. These provide independent correlative data necessary for pre-launch phase validation of Environmental Data Records (EDRs) derived from the NOAA Joint Polar Satellite System (JPSS) and Preparatory Project (NPP) (hereafter, JPSS) Cross-track Infrared Microwave Sounding Suite (CrIMSS),[1] and the NOAA Geostationary Operational Environmental Satellite R-series (GOES-R) Advanced Baseline Imager (ABI) (see Schmit et al. 2005, for details on ABI). Validation in the pre-launch phase is facilitated through the development of "proxy datasets," that is, sensor data approximated from existing satellite systems with similar specifications. Specifically, the planned low earth orbit (LEO) CrIMSS sounding system will be designed to operate in much the same manner as the Infrared Atmospheric Sounding Interferometer (IASI) (see Cayla 1993, for details on IASI) is paired with the Advanced Microwave Sounding Unit

[1]The CrIMSS consists of two passive sensors: the Cross Track Infrared Sounder (CrIS), a high resolution IR Fourier transform spectrometer (FTS), and the Advanced Technology Microwave Sounder (ATMS).

(AMSU-A) system onboard MetOp-A, as well as the Atmospheric Infrared Sounder system (AIRS/AMSU) onboard EOS-Aqua (see Chahine et al. 2006, for details on AIRS) in the NASA A-Train, including the scanning, cloud-clearing methodology, spectral/spatial resolution and coverage. Similarly, the GOES-R ABI will have spectral channels, temporal resolution and view geometry (e.g., Schmit et al. 2005) very close to the Spinning Enhanced Visible and Infrared Imager (SEVIRI) onboard Meteosat in geosynchronous earth orbit (GEO) (see Schmetz et al. 2002, for details on Meteosat). It is worth highlighting here that the AEROSE domain is well situated within the scanning range of SEVIRI, thus allowing for all sonde launches to be matched with SEVIRI fields-of-view (FOVs) (e.g., Nalli et al. 2008b).

Measurements over the open ocean are particularly valuable for cal/val (e.g., Hagan and Minnett 2003) given that the sea surface radiative properties (i.e., emission skin temperature and spectral emissivity/reflectivity) are well characterized and uniform (e.g., Smith et al. 1996; Nalli et al. 2006, 2008a), thus allowing these state parameters to be specified accurately. It is over open oceans, which constitute $\simeq$ 70% of the earth's surface area, where satellite data are expected to make their biggest impact on NWP. Furthermore, the multi-institutional and multidisciplinary nature of PNE/AEROSE allows for a "synergistic" approach to satellite cal/val: All collaborators benefit by gaining access to the various data, the broader science community (including actual and potential users of satellite products) is engaged, and NOAA's allocation of ship time onboard the *Ronald H. Brown* for PNE/AEROSE cruises is fully optimized.[2]

[2]It is an undeniable and oft understated cost-benefit to have a synergistic ocean/atmosphere campaign fully utilize the ship resource. For example, PNE/AEROSE does not waste fuel and resources during "transit

# 2. Overview of AEROSE Campaigns

As mentioned above, the geographic domain of AEROSE has been the Atlantic Ocean, primarily the tropical North Atlantic. Figure 2 shows the cruise tracks and times for the AEROSE domain to date; as can be seen, there is excellent coverage over most the domain. A brief summary of each cruise follows below.

*Cruise Summaries*

AEROSE-I, conducted during March 2004, was the main mission onboard the *Ronald H. Brown*, the details of which have been documented in earlier papers by (Nalli et al. 2005, 2006; Morris et al. 2006). The AEROSE mission objectives continued jointly as part the 2006 PNE/AEROSE-II cruise, initiated in conjunction with the 2006 African Monsoon Multidisciplinary Analysis (AMMA) (see Redelsperger et al. 2006, for details on AMMA), and successfully carried out in two 8-week legs during June–July 2006, as described in Morris et al. (2006) and Nalli et al. (2008a). The success of the 2006 campaign firmly established the PNE-AEROSE collaboration, and thus the PNE/AEROSE-III cruise followed in May 2007.

The fourth PNE/AEROSE campaign, scheduled for April–May 2008 (Cruise RB-08-03), with the port of origin being in Montevideo, Uruguay, has an unusual story behind its unique cruise track that requires some elaboration. Prior to the cruise, the *Ronald H. Brown* had been experiencing serious mechanical problems (brought on by a grueling yearly cruise schedule along with having to endure harsh sea conditions in the Southern Ocean for

legs" to buoys — it is precisely during these legs that some of the most valuable AEROSE data is collected.

the GasEx cruise prior). After the arrival of the scientific parties in Montevideo, departure was delayed by over 2-weeks and the cruise then severely descoped by the NOAA Office of Marine and Aviation Operations (OMAO) to assume a more direct track back to the United States (instead of eastward to 23°W, northward, then westward to Barbados, as originally planned). The descoped cruise track was charted to the west of the original track, and the PNE component of the mission was thereby canceled. However, the AEROSE team had already committed valuable time and resources (e.g., costs of shipment and travel to and from Uruguay), and thus decided to salvage whatever they could out of the RB-08-03 transit given that the descoped cruise track would nevertheless provide coverage in the Southern Hemisphere (SH) and some mid-basin in the Northern Hemisphere (NH). Unfortunately, additional problems led to progressive modifications in the track while under way, ultimately resulting in the ship remaining in the western Atlantic. Consequently, "PNE/AEROSE-IV" was never fully to be realized. In the end, in spite of these setbacks, the dedication on the part of the AEROSE team paid off: The resulting transit-campaign resulted in an interhemispheric transit resembling the Aerosols99 cruise, Jan–Feb 1999, from Norfolk, Virginia, USA to Capetown, South Africa (e.g., see Thompson et al. 2000; Bates et al. 2001; Voss et al. 2001, for more details on Aerosols99), albeit with sampling during boreal spring in the western, as opposed to eastern, South Atlantic.

The fifth and sixth campaigns, PNE/AEROSE-V and AEROSE-VI, were successfully executed as planned during July–August 2009 and late April–May, 2010, respectively. Each of these campaigns were somewhat unique in terms of sampling: The 2009 PNE/AEROSE occurred somewhat later in the summer, coinciding with the seasonal climatological peak of dust outflows, as well as during ramp up of the Atlantic hurricane season, whereas the 2010

cruise initiated out of Ghana, Africa, allowing for unique sampling of the Gulf of Guinea prior to the usual sampling of the tropical North Atlantic. The next PNE/AEROSE campaign is planned for spring 2011.

*Data Overview*

Through joint collaborations (see Acknowledgments), the AEROSE cruises have all been equipped with balloon-borne radiosondes and ozonesondes funded primarily to support the satellite validation objectives (discussed in Nalli et al. 2006), with launch times mostly coordinated to coincide with twice-daily LEO sounder overpasses (referred to as "dedicated sondes," launch times are scheduled $\simeq$ 0.5 h prior to a predicted overpass time at the ship location), namely the A-Train Aqua AIRS/AMSU, and starting in 2007, the MetOp IASI/AMSU. The AEROSE radiosonde observations (RAOBs) are obtained from commercial Vaisala rawinsondes (RS92-SGP, and in 2004, RS80-H and RS90) and include thermodynamic soundings of pressure, temperature and relative humidity (RH) (i.e., "PTU"). The Vaisala sondes also measure wind vectors via Global Positioning System (GPS), thus providing kinematic profiles of atmospheric winds (i.e., speed and direction),[3] with the RS92 sondes also providing geometric heights of measurement levels. Given that this last measurement (GPS heights) is obtained independent of the pressure sensor, this is valuable for validation of satellite derived pressure (a CrIMSS EDR) as a function of altitude levels. In addition to the RS92 PTU-wind soundings, EN-SCI Corporation ECC ozonesondes are interfaced (OIF92 interface) approximately once per day (launched $\simeq$1.0 h prior to the predicted overpass time) to provide ozone

[3]With the exception of the RS90 sondes launched near the end of the 2004 AEROSE-I.

profiles up through the lower stratosphere. Figure 3 charts the geographic locations and dates of the rawinsonde and ozonesonde launches. It can be seen that the PNE/AEROSE campaigns have attained multiple latitudinal and longitudinal Atlantic transects with RAOB frequencies that enable space-time cross-sectional analyses of temperature, moisture, winds and ozone as a function of altitude and ship coordinate. These profile cross-sections are presented and overviewed in Section 3.

The PNE/AEROSE cruises have also included Marine Atmospheric Emitted Radiance Interferometers (M-AERI) (see Minnett et al. 2001, for full details on M-AERI). These are ship-based FTS systems that measure well-calibrated (Revercomb et al. 1988), high-resolution radiance spectra (upwelling from the surface and downwelling from the atmosphere), usually at a height $\lesssim$10 m above sea level (Minnett et al. 2001). M-AERI data and analyses from the earlier 2004 and 2006 AEROSE-I and -II campaigns are reported in Nalli et al. (2006); Szczodrak et al. (2007); Nalli et al. (2008a); Martínez Avellaneda et al. (2010). From the M-AERI spectra, a number of critical geophysical state parameters can be derived, including high accuracy radiometric sea surface skin temperature, IR spectral emissivity (e.g., Smith et al. 1996; Hanafin and Minnett 2005; Nalli et al. 2008a), ambient air temperature (e.g., Smith et al. 1996; Minnett et al. 2005), and retrievals of boundary layer temperature and water vapor (e.g., Feltz et al. 1998; Szczodrak et al. 2007). Table 1 summarizes PNE/AEROSE "correlative data" germane for satellite EDR validation.

In addition to these data, a suite of other ship-based measurements are obtained during each AEROSE campaign. Microtops handheld sunphotometers provide multichannel observations of solar-spectrum aerosol optical depth (AOD), thereby providing a measure of column-integrated aerosols at the ship's location. Starting in 2009, AEROSE has collabo-

rated with the NASA/GSFC Maritime Aerosol Network (MAN) to apply the standardized methodology for maritime (ship-based) Microtops observations described in Smirnov et al. (2009), including sensor calibration, raw data processing and QA; AEROSE Microtops data prior to 2009 have been subsequently reprocessed using the MAN methodology. Multichannel $\tau_a(\lambda)$ for 2009–2010 are at $\lambda$ = 340, 380, 440, 500, 675, 870, 1020, 1640 nm; pre-2009 reprocessed multichannel data are at 339, 441, 674, 869 nm for years 2006–2008, and 340, 380, 870, 1020 nm for 2004. It should be noted that these measurements can be used as a correlative dataset for validating solar-spectrum satellite aerosol retrieval products. Ceilometers have also been deployed which provide observations of the cloud base height and rough estimates of the aerosol vertical distribution in the lower troposphere. *In situ* chemical, bulk aerosol and radiative surface data are also acquired, as reported in Morris et al. (2006). Thermo Electron Corporation (TECO) measurements include an ozone photometer (ambient gas-phase $O_3$), a CO IR spectrometer (ambient gas-phase CO), a $NO_x$ Chemilumen Analyzer (ambient NO and $NO_2$), and an $SO_2$ fluorometer (ambient gas-phase $SO_2$). Chemical, bulk and aerobiological sampling are obtained using quartz and Teflon filters. Condensation and laser particle counters measure surface aerosol number densities, and a Quartz Crystal Microbalance (QCM) cascade impactor measures surface aerosol mass densities. Finally, multiple independent broadband pyranometers and pyrgeometers operate to measure downwelling solar (visible) and terrestrial (IR) radiation for radiative energy balance calculations at the surface. Focused analyses of these data are subjects planned for future AEROSE-related papers.

# 3. Science Highlights

As already mentioned, the AEROSE study domain is a region of great meteorological interest, particularly when considering the mesoscale-observing missions of the GOES-R, CrIMSS, AIRS and IASI satellite observing systems. This section highlights some of the more salient phenomena captured by the PNE/AEROSE campaigns.

*Saharan Dust and Sub-Saharan Smoke*

In the troposphere, seasonally persistent elevated levels of aerosols with residence times >1 day are found to occur in regions downwind of continental sources. The main sources of these tropospheric aerosol include aeolian mineral dust from deserts, smoke from biomass burning and anthropogenic sources. Of these, dust from the Sahara Desert is the foremost source of global aerosols, which, along with the Arabian Desert, contributes a total mass of $\simeq$ 2000 Tg per annum, with particle sizes usually ranging from large to giant size $\bar{D} > 1$ $\mu$m(e.g., Hobbs 2000). Smoke from biomass burning sites (e.g., savanna grasslands in sub-Saharan Africa) contributes $\simeq$200–450 Tg per annum of biogenic aerosols of smaller, accumulation mode particles $\bar{D} \simeq 0.1$ $\mu$m. The massive and large-scale transport of dust and smoke from Africa across the Atlantic Ocean (the quantity of dust transport alone has been estimated at some 100–400 Tg per annum; Prospero et al. 1981) are the primary subjects of AEROSE.

The magnitude, extent and seasonal variation of trans-Atlantic African dust and smoke outflows are readily observed from space as in Figure 4, which shows a 22-year monthly AOD climatology (1981–2008 base period excluding the Mt. Pinatubo and El Chichón eruptions) for the tropical Atlantic Ocean and vicinity as derived from the NOAA Advanced Very High

Resolution Radiometer (AVHRR) Pathfinder Atmospheres Extended (PATMOS-x) dataset (e.g., Jacobowitz et al. 2003; Zhao et al. 2008). These data show first and foremost that Saharan dust outflows are, in a mean sense, a persistent feature of the North Atlantic atmosphere, even during months of minimal activity. A seasonal cycle is apparent in that the main dust plume axis translates northward (southward) during the boreal summer (winter) months, remaining to the north of the intertropical convergence zone (ITCZ). These trans-Atlantic dust outflows, in terms of westward extent and maximum intensity, also gradually decrease from a maximum during NH summer (Jun–Jul) to a minimum during the autumn (Oct–Nov) before increasing again in the spring, whereas dust outflows into the Gulf of Guinea become prevalent during the months of Dec–Mar (as noted by Resch et al. 2008). African smoke outflows associated with sub-saharan biomass burning gradually become apparent south of the ITCZ in the boreal spring before achieving a maximum in late summer (Jul–Sep), then gradually decreasing again, minimizing in winter. Biomass burning in Africa also occurs north of the ITCZ during boreal winter months, resulting in some contribution to the Atlantic and Gulf of Guinea plumes during Dec–Mar (e.g., Resch et al. 2008), and burning over the Yucatan Peninsula becomes prominent during Apr–May. Finally, there is also an the increase in aerosol outflows off the East Coast of the USA during spring to early autumn months (Mar–Sep), presumably the result of increased anthropogenic smog from the urban corridor.

Figures 5 and 6 show daily mean AEROSE column AOD, $\tau_a(\lambda)$, and derived Angstrom exponents, $\alpha = -\frac{\ln[\tau_a(\lambda_1)/\tau_a(\lambda_2)]}{\ln(\lambda_1/\lambda_2)}$, for meridional and zonal transects as measured from Microtops handheld sunphotometers and processed using the MAN methodology described by Smirnov et al. (2009). It is seen that the AEROSE campaigns have all encountered, to

varying degrees, aerosol plumes due to dust and smoke outflows from Africa. This includes persistently elevated levels near the African coast, as in the 2006 and 2009–2010 campaigns, as well as major dust pulses with AOD approaching or exceeding 1.0, as in the 2004 and 2007 campaigns. The multi-year measurements show patterns qualitatively consistent with the PATMOS-x climatology (Fig. 4) as well similar earlier field measurements from the Aerosols99 cruise (cf. Voss et al. 2001), generally corroborating the aerosol regimes observed by Bates et al. (2001). The zonal plots (Fig. 5) show a tendency toward lower AOD and higher $\alpha$ (smaller, non-dust particles) in the western North Atlantic basin, indicative of background marine aerosols (e.g., sea salt), or possibly industrial smoke and/or haze, as in 2010 (top left) or 2008 (Fig. 6, top left), which show slightly higher AOD. Encounters with dust plumes of varying degrees ($\tau_a \gtrsim 0.3$, $\alpha \lesssim 0.3$) become more prevalent eastward of 45°W, with the exception of 2010, during which the ship was cruising westward at $\simeq$13 kts under predominately westerly winds aloft. The meridional plots (Fig. 6), particularly those in the eastern Atlantic near the African coast, show persistently elevated aerosol levels associated with Saharan dust ($\tau_a \gtrsim 0.3$, $\alpha \lesssim 0.3$, typically north of the ITCZ), smoke from biomass burning ($\tau_a \gtrsim 0.3$, $\alpha \gtrsim 0.5$, typically south of the ITCZ), or some combination of both. The 2008 interhemispheric transit, top left, shows a small local peak in AOD at 10°N, $\tau_a \simeq 0.3$ and $\alpha \simeq 0.15$, these values being similar to that observed during Aerosols99 (cf. Voss et al. 2001), the result of remnant dust over the mid-Atlantic.

The dust pulse encountered during 2004 AEROSE-I (Fig. 5, bottom row left) was intense for the time of year (early March), and yet one of greater magnitude was encountered in May 2007 just prior to and during the northbound 23°W transect of PNE/AEROSE-III (Fig. 6, 2nd row left plot). Figure 7 shows a 13 May 2007 Meteosat SEVIRI color-composite RGB

image with the location and time of a concurrent radiosonde launch overlaid. It is seen that this sounding (Skew-T plot given below in Figure 9) was obtained within a very dusty, yet virtually cloud-free, air column well to the north of the ITCZ. For comparison, Figure 8 shows a nearly coincident digital color photograph of the dust outflow from the vantage point of the *Ronald H. Brown* while holding station along 23°W. The very low visibility near the horizon indicates the settling of dust into the surface layer of marine boundary layer (MBL), as also verified by concurrent ceilometer and PMS (data not shown here). Consistent with Figure 7, there are very few if any detectable low- to mid-level clouds within the camera FOV. We will return to this dust event in the overview-analysis of the entire complement of PNE/AEROSE RAOBs presented in the next subsection.

*The Saharan Air Layer (SAL) and the Distribution of Tropospheric Water Vapor*

The general distribution of tropical tropospheric RH is a topic of substantial concern, especially as it pertains to potential feedbacks in response to climate change (e.g., see Pierrehumbert and Roca 1998; Sherwood et al. 2006; Pierrehumbert et al. 2007; Dessler and Sherwood 2009), as well its impact upon tropical cyclogenesis and convection. Of particular interest over the tropical North Atlantic is the Saharan air layer (SAL), a stable layer of dry, warm air that often accompanies Saharan dust aerosols and advects across Atlantic basin, as first noted by Carlson and Prospero (1972). These conditions are believed to suppress hurricane activity over the Atlantic (e.g., Karyampudi and Pierce 2002; Dunion and Velden 2004; Wong and Dessler 2005; Evan et al. 2006; Wu 2007; Sun et al. 2008), and may also be self-sustaining as a result of reduced radiative cooling in the layer (e.g., Mapes and Zuidema

1996; Wong et al. 2009). While there have been a number of recent papers that have described the SAL based upon soundings over the region (e.g., Dunion and Marron 2008; Zipser et al. 2009), high-resolution *in situ* space-time cross-sections of the SAL were obtained for the first time over the eastern Atlantic basin from 3-hourly (8/day) RAOBs launched during the 2004 AEROSE-I campaign (as reported in Nalli et al. 2005). Hyper/ultraspectral sounding systems in LEO configuration (e.g., IASI/AIRS/CrIS), as well as geosynchronous imagers (e.g., ABI, SEVIRI), are valuable tools whereby the SAL and the distribution of tropospheric water vapor can be routinely observed in this manner (e.g., Pierrehumbert and Roca 1998; Dunion and Velden 2004; Zhang and Pennington 2004; Nalli et al. 2006; Sherwood et al. 2006), thus furthering the need for satellite validation correlative data in this region (e.g., Nalli et al. 2006; Wu 2009).

Figure 9 shows Skew-T Log-P diagrams of two sample soundings obtained from the PNE/AEROSE-III and -V campaigns alongside the recently published Dunion and Marron (2008) July–October mean tropical Caribbean sounding for SAL environments during hurricane season (Dunion and Marron 2008, hereafter, "DM08") for reference. The DM08 mean SAL sounding (far right) is the result of soundings obtained from stations in Miami, Grand Cayman, San Juan and Guadeloupe, spanning a region similar to that considered by Jordan (1958), during SAL conditions as ascertained from satellite. The leftmost Skew-T shows an AEROSE Caribbean RAOB launched 03:42 UTC 6 August 2009. This sounding was the final and westernmost sonde launch of the AEROSE-V campaign (18.75°N, 65.12°W), being launched immediately upon clearing the Barbuda Exclusive Economic Zone (EEZ), only $\simeq$105 km offshore from San Juan, Puerto Rico (18.45°N, 66.07°W). It is interesting to see striking similarity between this RAOB and the DM08 mean SAL sounding, in terms of

the location and strength of tropospheric dryness, the temperature profile, and prevailing easterly winds throughout the lower troposphere, although the fine scale variability, including moist filaments (cf. Pierrehumbert 1998; Pierrehumbert and Roca 1998), apparent in the AEROSE sounding has been lost in the smoothed mean sounding. It is probable that the driest layers in the AEROSE sounding above 600 hPa are associated, at least in part, with large-scale advection and subsidence drying in the Hadley circulation, this being consistent with the "advection-condensation" model formulated in a number of earlier papers such as Pierrehumbert and Roca (1998); Sherwood et al. (2006); Pierrehumbert et al. (2007).

The similarity between the two soundings, however, disappears altogether when we compare the RAOB from the eastern Atlantic (Figure 9, middle plot), a sonde launched along the 23°W south-north transect in the midst of intense dust outflow during the AEROSE-III campaign, 13:40 UTC 13 May 2007 (cf. Figures 7 and 8). In this sounding it is apparent that there are multiple dry layers, notably starting in the upper troposphere at 200–300 hPa, followed by a strong one at $\simeq$ 450 hPa, and a warm, moderately dry layer from 700 hPa down to the MBL inversion, with two embedded extremely dry filaments at 900 and 950 hPa. The multiple dry layers in this sounding are, generally speaking, all associated with well-defined inversions at their base (these characteristics also being observed by Mapes and Zuidema 1996), with temperatures in the low-level warm dry layer between 950 and 700 hPa substantially warmer than either the Caribbean sounding or the DM08 mean SAL sounding. It will be seen below in cross-sectional analyses that this RAOB is actually within the heaviest dust outflow to the north of the ITCZ and at the southern boundary of a very pronounced SAL extending well north of this location and reaching altitudes of 4 km. This case (as with the zonal cross-sections below) also suggests that another "tropical mean sounding," analogous

to Dunion and Marron (2008) and Jordan (1958), may in fact be desirable for the eastern Atlantic basin (as already hinted at by Dunion and Marron 2008); the full complement of AEROSE soundings may serve ideally for this purpose.

### Trans-Atlantic Cross-Sections: RH, VPTLR and Wind

As mentioned above, the RAOB launch frequency of each PNE/AEROSE campaign enables space-time cross-sectional analyses. As in Nalli et al. (2005), cross-sections are here generated by first preprocessing the sonde PTU data via least squares linear polynomial smoothing followed by linear interpolation to a common height coordinate. Figures 10–11 show the zonal cross-sections (longitude scales and transect subplot-ordering identical to Fig. 5) of tropospheric moisture (RH) and virtual potential temperature lapse rate (VPTLR), respectively. VPTLR is a direct indicator of local static stability (e.g., Stull 1991; Pan et al. 2009) defined as $\delta\theta_v(z)/\delta z$, where $\theta_v(z)$ is the virtual potential temperature sounding and $z$ is taken to be the geopotential height. Likewise, Figures 12–13 show the meridional cross-sections (latitude scales and transect subplot-ordering identical to Fig. 6) of RH and VPTLR, respectively.

While case-studies of the orthogonal cross-sections for specific campaigns can provide some insight on a given atmosphere's 4-D synoptic structure at mesoscale resolution, we attempt here only to highlight key features and patterns found in the ensemble zonal and meridional sections. The latitude zone of the ITCZ axis for each campaign can be seen clearly in Fig. 12, with a deep column of moist air extending from the surface up to the upper troposphere and what is presumably a divergence of moisture plumes northward and

southward at the top (e.g., Jun-06 and Jul-09, middle right plots). Beneath these moisture plumes flanking the ITCZ column are relatively deep layers of very dry air in the mid to upper troposphere (consistent with Mapes and Zuidema 1996; Pierrehumbert 1998; Pierrehumbert and Roca 1998; Sherwood et al. 2006), with relatively strong inversions present at their bases, probably resulting from net radiative heating as well as subsidence (as shown by Mapes and Zuidema 1996) and usually starting around 5 km as seen in Fig. 13.

Of particular interest to AEROSE is the SAL, which is seen to be a common feature in these cross-sections as low-level "filaments" or "tongues" (i.e., very shallow layers) of very dry air with very strong inversions just above the MBL on the north side of the ITCZ. Mapes and Zuidema (1996) asserted that such dry tongues within the tropical Pacific warm-pool atmosphere result mostly from advection, and indeed, it is our observation that the SAL appears merely to be a persistent special case of this "dry-tongue" phenomenon in the North Atlantic. The depth of the SAL appears to vary from extremely shallow (<1 km), but horizontally extensive (10–20°N) layers, as in May-10 (Fig. 12, top right), to deeper layers >2 km as in May-07 or Mar-04. Easterly winds are often, but not always, prevalent within the dry layer. The transects near the African coast show a stronger SAL (as measured by the VPTLR in Fig. 13) with the inversion base at very low altitudes, the lowest being the Mar-04 and May-07 cases. The Mar-04 transect was closest to the African coast, and indeed, the temperature inversion (MBL inversion strengthened by the SAL) begins immediately at the surface with the sharp discontinuity between moist MBL and dry SAL at $\simeq$0.2 km. The May-07 transect was highlighted above in the Skew-T plot of the 13:40 13-May-07 sounding launched at 9.50°N, 23.00°W (Fig. 9), and images of the concurrent dust plume from Meteosat (Fig. 7) and the *Ronald H. Brown* (Fig. 8). We may now see this isolated

sounding in its fuller context as located north of the ITCZ with the low-level dry filaments found at the southern lower edge of a prominent SAL extending from ≃0.35–4.0 km and 10°N to beyond 20°N, as well as a deep region of large-scale subsidence drying in the mid-to-upper levels, these both being associated with two strong inversions, one at the MBL interface and the other in the mid-troposphere around 5 km, features similar to those described by Mapes and Zuidema (1996). However, as mentioned above, the heaviest (daytime) dust outflow was observed at the ship location around 13-May-07 at ≃10°N (e.g., Figs. 7, 8, and 6, middle left plot), thereby presenting a case where the driest air column does not necessarily coincide with the heaviest dust loading (as also observed by Zhang and Pennington 2004). Finally, the two interhemispheric cross-sections, the Apr-May 2008 RB-08-03 (top left) and Jan-Feb Aerosols99 (lower right), in spite of the differing seasons, sampling of the east and west South Atlantic basin, and higher resolution of the AEROSE soundings, have some similarities, specifically the location of what appears to be a dry air mass north of the ITCZ around 10°N (although drier air was observed at a lower altitude during the 2008 campaign).

The zonal cross-sections shown in Figs. 10–11 were all obtained, with the exception of the 2010 Gulf of Guinea E-W transect (lower right plots) and the 2007 W-E and 2006 Leg 1 E-W transects (not shown due to space limitations), to the north of the ITCZ. With the exception of isolated areas of obvious convection extending from the surface upward and moist plumes aloft, these cross-sections show dry air at mid-to-upper levels (generally >3 km), with well-defined inversions at their bases, spanning much of the tropical to sub-tropical North Atlantic basin. These are not necessarily Saharan in origin, but may also be the result of large-scale subsidence associated with Hadley circulation (cf. Sherwood et al. 2006), or large-scale advection from elsewhere in the sub-tropics (cf. Mapes and Zuidema 1996). As

above, the SAL is thus believed to be confined mostly to levels sandwiched between the MBL and $\simeq$5 km. If we turn to the VPTLR cross-sections (Fig. 11) and assume strong VPTLR above the MBL results from advection of Saharan (dry, warm) air at low levels that is radiatively maintained or strengthened (as reported by Mapes and Zuidema 1996; Wong et al. 2009), then we may infer SALs were present, to varying degrees and extents, in all the transects (with the obvious exception of the Gulf of Guinea), some extending as far as 50°W.

*Tropospheric Ozone Dynamics*

The "tropical Atlantic ozone paradox" and "zonal wave-one" are related tropospheric phenomena that have been the subject of considerable recent research (e.g., Jonquières et al. 1998; Thompson et al. 2000, 2003; Jenkins and Ryu 2004; Sauvage et al. 2006; Ziemke et al. 2006; Jourdain et al. 2007; Jenkins et al. 2008). Roughly speaking, the term "paradox" refers to an unexpected seasonal periodic behavior in free tropospheric $O_3$ over the tropical North and South Atlantic, assuming tropospheric ozone formation from ozone precursors arising from biomass burning.

Whereas the full nature of this phenomenon does not appear to be completely understood, it is the observation of higher tropospheric $O_3$ in the SH during the NH burning season over the tropical Atlantic that has been considered "paradoxical" (cf. Thompson et al. 2003; Sauvage et al. 2006; Jourdain et al. 2007). In addition to the apparent paradox, the observed seasonal variation in the tropical-zonal distribution of tropospheric ozone, at least in the SH, has been described as a "zonal wave-one" (e.g., Thompson et al. 2000, 2003; Ziemke et al.

2006), with the ridge axis occurring over the mid-South Atlantic, maximum amplitude occurring in September–November (SON), and a trough (presumably) located over the Pacific Ocean (cf. Sauvage et al. 2006; Ziemke et al. 2006; Jourdain et al. 2007). Based upon satellite and limited *in situ* data records, the tropical $O_3$ wave-one and associated Atlantic paradox have been described as "a common Atlantic feature" and "a predominantly SH phenomenon" (Sauvage et al. 2006), even though biomass "burning in the northern and southern Africa tropical belts is very similar" (Jonquières et al. 1998).

During the Aerosols99 interhemispheric cruise, Thompson et al. (2000) noted that the highest SH tropospheric $O_3$ is observed from both *in situ* ozonesonde and satellites during boreal autumn, 2-3 months after peak regional biomass burning. Jenkins and Ryu (2004) extended the "Atlantic paradox" conceptual model to the NH by observing that seasonally elevated total column ozone (TCO) values in the NH (SH) occur during the periods of SH (NH) biomass burning. They attributed this behavior primarily to $NO_x$ formation (an $O_3$ precursor) arising from seasonally consistent lightning patterns in central and western Africa, followed by advection via easterly winds. Monthly charts of satellite-derived TCO published by Ziemke et al. (2006) also show the transition of elevated zonal TCO from the SH to the NH during the seasonal march from SON to JJA, and that this behavior is not isolated to the Atlantic. Jourdain et al. (2007), considering the vertical distribution, noted that there are actually "two maxima: one in the lower troposphere north of the ITCZ and one in the middle and upper troposphere south of the ITCZ"; this feature was, in fact, also observed during the Aerosols99 campaign. The studies overviewed here are nearly unanimous in their assessment that the ozone wave-one and Atlantic paradox (when observed) are likely the product of three different sources: $O_3$ precursors from biomass

burning and lightning, and stratosphere-troposphere exchange (STE), sometimes referred to as "stratospheric intrusions" (e.g., Pan et al. 2009).

### Trans-Atlantic Cross-Sections: Ozone and Wind

The combined AEROSE campaign ozonesonde data have resulted in the most extensive *in situ* soundings of atmospheric ozone profiles over the tropical Atlantic ever attempted (see Table 1). Like the PTU soundings, the ozonesondes are of sufficient frequency to perform trans-Atlantic cross-sectional analyses. Figure 14 shows the zonal ozone cross-sections for AEROSE zonal transects shown previously (where applicable, the longitude scales and transect subplot-ordering correspond to that in Figs. 5, 10 and 11). Likewise, Figure 15 shows the meridional cross-sections for transects shown previously, with the ozone cross-section from the Aerosols99 cruise (described in Thompson et al. 2000) also shown (lower right) for reference (again, latitude scales and transect subplot-ordering corresponding to Figs. 6, 12 and 13 where applicable).

Generally speaking, mid- to high-level tropospheric ozone concentrations correlate with the dry layers (notably excluding SALs) seen in Figs. 10 and 15. The meridional cross-sections are of particular interest in terms of how they may resemble and/or differ from the earlier Aerosols99 "baseline" (Fig. 15, lower right). The AEROSE 2008 RB-08-03 interhemispheric transect (Fig. 15, upper left) is the most similar in terms of cruise track (Fig. 3), although AEROSE/RB-08-03 (Aerosols99) was during boreal spring (winter) and sampled the western (eastern) South Atlantic at lower (higher) horizonal resolution. Most notable when comparing these two cross-sections is what appears to be a "reversal" in the mid-level

tropospheric ozone (5–10 km), with the May-08 data showing elevated $O_3$ in the NH, between 15–30°N, instead of the SH between 0–23°S, as in Jan-99. The low-level (0–5 km) $O_3$ concentrations, on the other hand, show more similarity. The remaining AEROSE NH cross-sections are arranged in mean ordinal date order from top to bottom, the two following the 2008 section (2010 and 2007, respectively) also during the month of May, show similar ozone concentrations and patterns as the 2008 NH data. The final three cross-sections, spanning early to mid-summer, appear to show a trend toward increasing amounts of NH mid- to upper-tropospheric ozone. Furthermore, elevated mid-to-upper tropospheric NH $O_3$ is seen to span much of the tropical North Atlantic during these periods, as seen in Fig. 14. These observations thus seem to corroborate earlier observations of a NH $O_3$ maximum in JJA (e.g., Jenkins and Ryu 2004; Ziemke et al. 2006; Jenkins et al. 2008).

To provide some context on the 2008 measurements, Fig. 16 shows PATMOS-x AVHRR May 2008 mean 0.63 $\mu$m $\tau_a$ and derived $\alpha$, the May 2008 Moderate Resolution Imaging Spectroradiometer (MODIS) fire product (see Giglio et al. 2003, for more details on the MODIS fire product), and the ECMWF 860 hPa wind and total precipitable water (TPW) fields for 2–18 May. We note well-known regions of significant biomass burning typically occurring this time of year evident in the MODIS Fire Product (lower left plot), including African savannas between 0–20°S and 15–30°E as well as the Yucatan Peninsula. There are also some regions with less-intense burning including the vicinity of Senegal as well as regions in South America, particularly Venezuela. The smoke emissions of these burning sites are clearly manifest in the PATMOS-x $\tau_a$ and $\alpha$ (top left and right, respectively), especially $\alpha$.

Now considering the 2008 AEROSE transit data, the cruise track (Fig. 16, lower left) passes from a region of background marine aerosols with $\tau_a \simeq 0.1$ south of the ITCZ to

a region of increasing $\tau_a$ and $\alpha$ (starting around 9 May) north of it. This is seen in the AVHRR $\tau_a$, $\alpha$ and ECMWF model TPW (Fig. 16 upper and lower right plots, respectively) as well as the Microtops measurements onboard the *Ronald H. Brown* (Fig. 6, top left). As mentioned above, the ship first passes through the main trans-Atlantic plume around 10°N. Following this peak, we see a gradual increase in $\tau_a$ from $\simeq$0.1 to 0.2 with an attendant increase in Microtops $\alpha$ from $\simeq$0.2 to 0.6, leading one to suspect an increase in smaller-mode aerosols characteristic of smoke and/or industrial haze. NOAA HYSPLIT model 96 h back trajectories (not shown due to space limitations) ending at ozonesonde launches in the vicinity of 10°N confirm tropospheric parcels originating from Africa along the main dust plume axis, but for launches to the north of this at $\simeq$15°N the trajectories shift to origins out of the Caribbean Sea, the Gulf of Mexico and North America. These observations are consistent with the hypothesis of tropospheric ozone formation from CO precursors present in smoke outflows possibly originating from biomass burning (e.g., from the Yucatan and Caribbean) or possibly anthropogenic smog from the USA east coast urban corridor. Regarding the lower concentrations of SH tropospheric $O_3$ seen in our data, especially as compared to Aerosols99, despite the significant savanna biomass burning in Africa (Fig. 16, lower left) the smoke plume simply does not extend to the western Atlantic (Fig. 16, top plots), possibly being advected northward into the ITCZ within the monsoonal flow (cf. Jonquières et al. 1998). More focused study on the AEROSE ozone measurements, both sonde and surface-based, is to be the subject of future work.

# 4. Summary

This paper has provided an overview of the NOAA Aerosols and Ocean Science Expeditions (AEROSE), trans-Atlantic intensive campaigns begun in 2004 and conducted yearly since 2006 in collaboration with the PIRATA Northeast Extension (PNE) project. Science topics germane to the tropical Atlantic atmosphere were highlighted, particularly micro-, meso- and synoptic-scale marine phenomena related to air mass outflows from Africa and other continental regions. It was noted that advanced environmental satellite observing systems both current (e.g., IASI/AMSU and AIRS/AMSU) and future (e.g., the JPSS CrIMSS and GOES-R ABI) are designed for the observation of such phenomena, thus requiring validation of EDR products under such conditions over open ocean. To this end, attention was given to a unique compilation of multi-year atmospheric *in situ* temperature, water vapor, wind and ozone profiles derived from dedicated balloon-borne radiosondes launched to coincide with overpasses of the NASA A-Train Aqua and EUMETSAT MetOp satellites. The sonde launch frequencies during each campaign allow for unique multi-year zonal and meridional cross-sectional analyses of the tropical Atlantic, and as such are valuable for study of African dust and smoke aerosol outflows, the associated SAL and distribution of tropical water vapor, the dynamics of tropospheric ozone, as well as providing the correlative data necessary for satellite validation (viz., CrIMSS, GOES-R), this latter work to be the subject of future papers.

Fortuitously, NOAA has been committed to maintaining the PNE array and has thereby supported yearly PNE/AEROSE cruises, which are slated to continue through at least 2011, thereby potentiating at least one more campaign, currently planned for the spring.

PNE/AEROSE campaigns beyond 2011 are less certain, but nevertheless would contribute to the current unprecedented data complement, and would also potentially provide the platform for acquiring open-ocean correlative data for the Intensive Cal/Val phase of CrIMSS EDR products following the tentative launch of the NPP satellite in 2012.

*Acknowledgments.*

This research has been supported by the NOAA Educational Partnership Program grant NA17AE1625, NOAA grant NA17AE1623 to establish NCAS, the STAR Satellite Meteorology and Climatology Division (SMCD) and GOES-R Algorithm Working Group (M. D. Goldberg, SMCD Division Chief), the NOAA Integrated Program Office (2008–2010), the Joint Center for Satellite Data Assimilation FY05-06 Science Development and Implementation Task, and the NASA AIRS Science Team (2006–2008). Funding for PNE is provided by NOAA's Office of Climate Observations (Climate Program Office).

Predictions for LEO satellite overpasses were made possible via the orbit prediction utility developed by L. Nguyen and can be accessed at the NASA Langley Clouds and Radiation Group webpage, http://www-angler.larc.nasa.gov. The NOAA Air Resources Laboratory (ARL) is acknowledged for the provision of the HYSPLIT transport and dispersion model and/or READY website (http://www.arl.noaa.gov/ready.html) used in this publication. The AVHRR PATMOS-x climate data was developed by A. Heidinger et al. (STAR, UW-Madison) and made available for download on the PATMOS-x project webpage http://cimss.ssec.wisc.edu/patmosx/. The AMMA program is a French initiative built by an international scientific group and funded by a large number of agencies, especially from

France, UK, USA and Africa.

We are grateful to to numerous individuals who supported or contributed to AEROSE over the years: P. Clemente-Colón (NESDIS/STAR National Ice Center), who was the Chief Scientist of AEROSE-I, and C. Schmid (NOAA/AOML), the 2010 PNE Chief Scientist; T. King (DSFG), for IASI data acquisition and processing support; T. Zhu (CSU/CIRA) for GOES-R proxy data support; C. Dean (QSS/PSGS Program Manager); T. Pagano (JPL), and W. Feltz, R. Knuteson (UW/CIMSS), for sonde support; T. Schmit and J. Li (UW/CIMSS GOES-R Soundings Team); and G. Jenkins (Howard U.) for AMMA collaboration. Cruise participants who supported sonde operations include E. Roper (Lincoln U.), and R. Armstrong and Y. Detrés (UPRM). We also acknowledge the many students who assisted in and facilitated the collection data throughout the cruises (too numerous to list completely here), especially Howard University students A. Flores (Microtops and post-cruise data management), C. Stearns (ozonesonde prep and sonde inventory), L. Roldán and M. Hawkins (early AEROSE). Finally, we extend our appreciation to all the crew and officers of the *Ronald H. Brown* for their support throughout the years. The views, opinions, and findings contained in this report are those of the authors and should not be construed as an official NOAA or U.S. Government position, policy, or decision.

# REFERENCES


Bates, T. S., et al., 2001: Regional physical and chemical properties of the marine boundary layer aerosol across the Atlantic during Aerosols99: An overview. *J. Geophys. Res.*, **106 (D18)**, 20 767–20 782.

Bourlès, B., et al., 2008: The PIRATA program: History, accomplishments, and future directions. *Bull. Amer. Meteorol. Soc.*, **89 (8)**, 1111–1125, doi/10.1175/2008BAMS2462.1.

Carlson, T. N. and J. M. Prospero, 1972: The large-scale movement of Saharan air outbreaks over the northern equatorial Atlantic. *J. Appl. Meteor.*, **11**, 283–297.

Cayla, F. R., 1993: IASI infrared interferometer for operations and research. *NATO ASI Series*, S. Chedin, Chahine, Ed., Springer-Verlag, Berlin Heidelberg, I, Vol. 19, 9–19.

Chahine, M. T., et al., 2006: AIRS: Improving weather forecasting and providing new data on greenhouse gases. *Bull. Am. Meteorol. Soc.*, **87 (7)**, 911–926.

Dessler, A. E. and S. C. Sherwood, 2009: A matter of humidity. *Science*, **323**, 1020–1021.

Dunion, J. P. and C. S. Marron, 2008: A reexamination of the Jordan mean tropical sounding based on awareness of the Saharan air layer: Results from 2002. *J. Climate*, **21 (10)**, 5242–5253.

Dunion, J. P. and C. S. Velden, 2004: The impact of the Saharan air layer on Atlantic tropical cyclone activity. *Bull. Am. Meteorol. Soc.*, **85 (3)**, 353–385.

Evan, A. T., J. Dunion, J. A. Foley, A. K. Heidinger, and C. S. Velden, 2006: New evidence for a relationship between Atlantic tropical cyclone activity and African dust outbreaks. *Geophys. Res. Lett.*, **33**, l19813, doi:10.1029/2006GL026408.

Feltz, W. F., W. L. Smith, R. O. Knuteson, H. E. Revercomb, H. M. Woolf, and H. B. Howell, 1998: Meteorological applications of temperature and water vapor retrievals from the ground-based Atmospheric Emitted Radiance Interferometer (AERI). *J. Appl. Meteor.*, **37**, 857–875.

Giglio, L., J. Descloitres, C. O. Justice, and Y. J. Kaufman, 2003: An enhanced contextual fire detection algorithm for MODIS. *Remote Sens. Environ.*, **87**, 273–282.

Hagan, D. E. and P. J. Minnett, 2003: AIRS radiance validation over ocean from sea surface temperature measurements. *IEEE Trans. Geosci. Remote Sensing*, **41 (2)**, 432–441.

Hanafin, J. A. and P. J. Minnett, 2005: Measurements of the infrared emissivity of a wind-roughened sea surface. *Appl. Optics*, **44 (3)**, 398–411.

Hobbs, P. V., 2000: *Introduction to Atmospheric Chemistry*. Cambridge University Press, New York, NY, 262 pp.

Jacobowitz, H., L. L. Stowe, G. Ohring, A. Heidinger, K. Knapp, and N. R. Nalli, 2003: The advanced very high resolution radiometer Pathfinder Atmosphere (PATMOS) climate dataset: A resource for climate research. *Bull. Amer. Meteorol. Soc.*, **84 (6)**, 785–793.

Jenkins, G. S., M. Camara, and S. A. Nidaye, 2008: Observational evidence of enhanced middle/upper tropospheric ozone via convective processes over the equatorial tropical Atlantic during the summer of 2006. *Geophys. Res. Lett.*, **35**, L12 806, doi:10.1029/2008GL033 954.

Jenkins, G. S. and J. H. Ryu, 2004: Space-borne observations link the tropical atlantic ozone maximum and paradox to lightning. *Atmos. Chem. Phys.*, **4**, 361375.

Jonquières, I., A. Marenco, A. Maalej, and F. Rohrer, 1998: Study of ozone formation and transatlantic transport from biomass burning emissions over West Africa during the airborne Tropospheric Ozone Campaigns TROPOZ I and TROPOZ II. *J. Geophys. Res.*, **103 (D15)**, 19,059–19,073.

Jordan, C. L., 1958: Mean soundings for the West Indies area. *J. Meteor.*, **15**, 91–97.

Jourdain, L., et al., 2007: Tropospheric vertical distribution of tropical Atlantic ozone observed by TES during the northern African biomass burning season. *Geophys. Res. Lett.*, **34**, L04 810, doi:10.1029/2006GL028 284.

Kahn, R. A., et al., 2004: Aerosol data sources and their roles within PARAGON. *Bull. Amer. Meteorol. Soc.*, **85 (10)**, 1511–1522.

Karyampudi, V. M. and H. F. Pierce, 2002: Synoptic-scale influence of the Saharan air layer on tropical cyclogenesis over the eastern Atlantic. *Monthly Weather Rev.*, **130**, 3100–3128.

Mapes, B. E. and P. Zuidema, 1996: Radiative-dynamical consequences of dry tongues in the tropical atmosphere. *J. Atmos. Sci.*, **53 (4)**, 620–638.

Martínez Avellaneda, N., N. Serra, P. J. Minnett, and D. Stammer, 2010: Response of the eastern subtropical Atlantic SST to Saharan dust: A modeling and observational study. *J. Geophys. Res.*, **115**, C08 015, doi:10.1029/2009JC005 692.

Minnett, P. J., R. O. Knuteson, F. A. Best, B. J. Osborne, J. A. Hanafin, and O. B.

Brown, 2001: The Marine-Atmospheric Emitted Radiance Interferometer (M-AERI): a high-accuracy, sea-going infrared spectroradiometer. *J. Atmos. Oceanic Tech.*, **18**, 994–1013.

Minnett, P. J., K. A. Maillet, J. A. Hanafin, and B. J. Osborne, 2005: Infrared interferometric measurements of the near surface air temperature over the oceans. *J. Atmos. Ocean. Tech.*, **22**, 1019–1032.

Morris, V., E. Joseph, S. Smith, , and T.-W. Yu, 2010: The Howard University Program in Atmospheric Sciences (HUPAS): A program exemplifying diversity and opportunity. *J. Geosci. Edu.*, submitted.

Morris, V., T.-W. Yu, E. Joseph, R. Armstrong, R. Fitzgerald, R. Karim, X.-Z. Liang, and Q. Min, 2007: The NOAA Center for Atmospheric Sciences (NCAS): Programs and achievements. *Bull. Am. Meteorol. Soc.*, **88 (2)**, 141–145.

Morris, V., et al., 2006: Measuring trans-Atlantic aerosol transport from Africa. *Eos Trans. AGU*, **87 (50)**, 565–571.

Nalli, N. R., P. J. Minnett, E. Maddy, W. W. McMillan, and M. D. Goldberg, 2008a: Emissivity and reflection model for calculating unpolarized isotropic water surface leaving radiance in the infrared. 2: Validation using Fourier transform spectrometers. *Appl. Optics*, **47 (25)**, 4649–4671.

Nalli, N. R. and L. L. Stowe, 2002: Aerosol correction for remotely sensed sea surface temperatures from the National Oceanic and Atmospheric Administration advanced very high resolution radiometer. *J. Geophys. Res.*, **107 (C10)**, 3172, doi:10.1029/2001JC001 162.

Nalli, N. R., H. Xie, C. D. Barnet, and M. D. Goldberg, 2008b: Using AEROSE-domain SEVIRI data for legacy sounding products from the GOES-R Advanced Baseline Imager. *Proc. 2008 EUMETSAT Meteorological Satellite Conf.*, Darmstadt, Germany, EUMETSAT, Vol. EUM P.52, iSBN 978-92-9110-082-8, ISSN 1011-3932.

Nalli, N. R., et al., 2005: Profile observations of the Saharan air layer during AEROSE 2004. *Geophys. Res. Lett.*, **32**, L05815, doi:10.1029/2004GL022028.

Nalli, N. R., et al., 2006: Ship-based measurements for infrared sensor validation during Aerosol and Ocean Science Expedition 2004. *J. Geophys. Res.*, **111**, D09S04, doi:10.1029/2005JD006 385.

Pan, L. L., et al., 2009: Tropospheric intrusions associated with the secondary tropopause. *J. Geophys. Res.*, **114**, D10 302, doi:10.1029/2008JD011 374.

Pierrehumbert, R. T., 1998: Lateral mixing as a source of subtropical water vapor. *Geophys. Res. Lett.*, **25 (2)**, 151–154.

Pierrehumbert, R. T., H. Brogniez, and R. Roca, 2007: *The Global Circulation of the Atmosphere*, chap. 6. On the relative humidity of the atmosphere, 400 pp. Princeton.

Pierrehumbert, R. T. and R. Roca, 1998: Evidence for control of Atlantic subtropical humidity by large scale advection. *Geophys. Res. Lett.*, **25 (24)**, 4537–4540.

Prospero, J. M., R. A. Glaccum, and R. T. Nees, 1981: Atmospheric transport of soil dust from Africa to South America. *Nature*, **289**, 570–572.

Redelsperger, J.-L., C. D. Thorncroft, A. Diedhiou, T. Lebel, D. J. Parker, and J. Polcher,

2006: African monsoon multidisciplinary analysis: An international research project and field campaign. *Bull. Amer. Meteorol. Soc.*, **87 (12)**, 1739–1746.

Resch, F., A. Sunnu, and G. Afeti, 2008: Saharan dust flux and deposition rate near the Gulf of Guinea. *Tellus*, **60B**, 98105.

Revercomb, H. E., H. Buijs, H. B. Howell, D. D. LaPorte, W. L. Smith, and L. A. Stromovsky, 1988: Radiometric calibration of IR Fourier transform spectrometers: Solution to a problem with the high-resolution interferometer sounder. *Appl. Opt.*, **27 (15)**, 3210–3218.

Robinson, L., J. Rousseau, D. Mapp, V. Morris, and M. Laster, 2008: An Educational Partnership Program with Minority Serving Institutions: A framework for producing minority scientists in NOAA-related disciplines. *J. Geosci. Edu.*, **55 (6)**, 486–492.

Sauvage, B., V. Thouret, A. M. Thompson, J. C. Witte, J.-P. Cammas, P. Nédélec, and G. Athier, 2006: Enhanced view of the "tropical Atlantic ozone paradox" and zonal wave one" from the in situ MOZAIC and SHADOZ data. *J. Geophys. Res.*, **111**, D01 301, doi:10.1029/2005JD006 241.

Schmetz, J., P. Pili, S. Tjemkes, D. Just, J. Kerkmann, S. Rota, and A. Ratier, 2002: An introduction to Meteosat Second Generation (MSG). *Bull. Am. Meteorol. Soc.*, **83 (7)**, 977–992.

Schmit, T. J., M. M. Gunshor, W. P. Menzel, J. J. Gurka, J. Li, and A. S. Bachmeier, 2005: Introducing the next-generation advanced baseline imager on GOES-R. *Bull. Am. Meteorol. Soc.*, **86 (8)**, 1079–1096.

Sherwood, S. C., E. R. Kursinski, and W. G. Read, 2006: A disribution law for free-tropospheric relative humidity. *J. Climate*, **19**, 6267–6277.

Smirnov, A., et al., 2009: Maritime Aerosol Network as a component of Aerosol Robotic Network. *J. Geophys. Res.*, **114**, D06 204, doi:10.1029/2008JD011 257.

Smith, W. L., et al., 1996: Observations of the infrared properties of the ocean: Implications for the measurement of sea surface temperature via satellite remote sensing. *Bull. Am. Meteorol. Soc.*, **77**, 41–51.

Stowe, L. L. and H. E. Fleming, 1980: The error in satellite retrieved temperature profiles due to the effects of atmospheric aerosol particles. *Rem. Sens. Environ.*, **9**, 57–64.

Stull, R. B., 1991: Static stability—an update. *Bull. Amer. Meteorol. Soc.*, **72 (10)**, 1521–1529.

Sun, D., K. M. Lau, and M., 2008: Contrasting the 2007 and 2005 hurricane seasons: Evidence of possible impacts of Saharan dry air and dust on tropical cyclone activity in the Atlantic basin. *Geophys. Res. Lett.*, **35**, L15 405, doi:10.1029/2008GL034 529.

Szczodrak, M., P. J. Minnett, N. R. Nalli, and W. F. Feltz, 2007: Profiling the lower troposphere over the ocean with infrared hyperspectral measurements of the Marine-Atmosphere Emitted Radiance Interferometer. *J. Atmos. Ocean. Tech.*, **34 (3)**, 390–402.

Thompson, A. M., et al., 2000: A Tropical Atlantic paradox: Shipboard and satellite views of a tropospheric ozone maximum and wave-one in January-February 1999. *Geophys., Res. Lett.*, **27 (20)**, 3317–3320.

Thompson, A. M., et al., 2003: Southern Hemisphere Additional Ozonesondes (SHADOZ) 19982000 tropical ozone climatology 2. Tropospheric variability and the zonal wave-one. *J. Geophys. Res.*, **108 (D2)**, 8241, doi:10.1029/2002JD002 241.

Voss, K. J., E. J. Welton, P. K. Quinn, R. Frouin, M. Miller, and R. M. Reynolds, 2001: Aerosol optical depth measurements during the Aerosols99 experiment. *J. Geophys. Res.*, **106 (D18)**, 20 811–20 819.

Weaver, C. J., J. Joiner, and P. Ginoux, 2003: Mineral aerosol contamination of TIROS Operational Vertical Sounder (TOVS) temperature and moisture retrievals. *J. Geophys. Res.*, **108 (D8)**, 4246, doi:10.1029/2002JD002571.

Wong, S. and A. E. Dessler, 2005: Suppressiong of deep convection over the tropical North Atlantic by the Saharan air layer. *Geophys. Res. Lett.*, **32**, L09808, doi:10.1029/2004GL022295.

Wong, S., A. E. Dessler, N. M. Mahowald, P. Yang, and Q. Feng, 2009: Maintenance of lower tropospheric temperature inversion in the Saharan air layer by dust and dry anomaly. *J. Climate*, **22 (10)**, 5149–5162.

Wu, L., 2007: Impact of saharan air layer on hurricane peak intensity. *Geophys. Res. Lett.*, **34**, L09 802, doi:10.1029/2007GL029 564.

Wu, L., 2009: Comparison of atmospheric infrared sounder temperature and relative humidity profiles with NASA African Monsoon Multidisciplinary Analyses (NAMMA) dropsonde observations. *J. Geophys. Res.*, **114**, d19205, doi:10.1029/2009JD012083.

Zhang, C. and J. Pennington, 2004: African dry air outbreaks. *J. Geophys. Res.*, **109 (D20108)**, doi:10.1029/2003JD003 978.

Zhao, X.-P., I. Laszlo, W. Guo, A. Heidinger, C. Cao, A. Jelenak, D. Tarpley, and J. Sullivan, 2008: Study of long-term trend in aerosol optical thickness observed from operational AVHRR satellite instrument. *J. Geophys. Res.*, **113 (D07201,)**, doi:10.1029/2007JD009 061.

Ziemke, J. R., S. Chandra, B. N. Duncan, L. Froidevaux, P. K. Bhartia, P. F. Levelt, and J. W. Waters, 2006: Tropospheric ozone determined from Aura OMI and MLS: Evaluation of measurements and comparison with the Global Modeling Initiatives Chemical Transport Model. *J. Geophys. Res.*, **111**, D19 303, doi:10.1029/2006JD007 089.

Zipser, E. J., et al., 2009: The Saharan air layer and the fate of African easterly waves: NASAs AMMA field study of tropical cyclogenesis. *Bull. Am. Meteorol. Soc.*, **90 (8)**, 1137–1156.

# List of Tables

TABLE 1. AEROSE Tropical Atlantic Satellite Cal/Val Correlative Data (2004, 2006–2010).

| Dates | Vaisala radiosondes[1] | | EN-SCI ECC ozonesondes[1] | | M-AERI[2] | Microtops[3] |
|---|---|---|---|---|---|---|
| 2004 Mar | 156 | (42, 0) | 0 | (0, 0) | 24 | 21 |
| 2006 Jun–Jul | 96 | (69, 0) | 20 | (18, 0) | 37 | 28 |
| 2007 May | 96 | (40, 43) | 17 | (7, 10) | 24 | 18 |
| 2008 Apr–May | 74 | (33, 34) | 16 | (8, 8) | 23 | 10 |
| 2009 Jul–Aug | 81 | (32, 33) | 17 | (8, 9) | 0 | 17 |
| 2010 Apr–May | 75 | (36, 38) | 19 | (10, 9) | 24 | 19 |
| Totals | 578 | (252, 148) | 89 | (51, 36) | 132 | 113 |

[1] Successful launches; numbers in parentheses denote launches timed for Aqua/A-Train and MetOp overpasses, respectively. Vaisala RS92-SGP (GPS) radiosondes have been used for all campaigns except in 2004, which used RS80-H (GPS) and RS90 (non-GPS). In 2006 and 2007 some sondes were uploaded into the Global Telecommunications System for numerical forecast model assimilation in cooperation with the AMMA program; in all other cases, AEROSE sondes were not assimilated.

[2] Number of days with available quality-assured (QA) data; in 2009 the M-AERI suffered from unexpectedly high levels of instrument spectral random noise.

[3] Number of days measurements were taken; 2009–2010 data include MAN calibrated-QA 8-channel AODs.

# List of Figures

5 Microtops sunphotometer daily mean AOD ($\tau_a$, blue) and derived Angstrom exponents ($\alpha$, red) for zonal AEROSE transects plotted on a common longitude scale. Small numbers above the main $x$-axis labeling denote the limits of the orthogonal axis (i.e., latitude). Raw AOD values have been processed according to the Maritime Aerosol Network (MAN) methodology (Smirnov et al. 2009). The plots are roughly "sorted" from left-to-right, top-to-bottom as north to south zonal sections. 51

6 As Figure 5 except for meridional AEROSE transects plotted on a common latitude scale. Small numbers above the main $x$-axis labeling denote the limits of the orthogonal axis (i.e., longitude). The plots are roughly "sorted" from left-to-right, top-to-bottom as first west to east meridional sections and then time of the year. 52

7 SEVIRI RGB color-composite (using channels 1.6 $\mu$m, 0.8 $\mu$m and 0.6 $\mu$m for red, green and blue, respectively) 2-km imagery for the AEROSE domain, 13:12 UTC, 13 May 2007. The location of a coincident sonde launch (9.501°N, 22.998°W; 13:40 UTC) within a strong Saharan dust outflow plume (cf. Figure 9) is shown in yellow. Map projection is vertical perspective azimuthal. NESDIS/STAR has archived hourly 2-km SEVIRI multichannel data for all the AEROSE campaigns to create a marine-based GOES-R proxy dataset for pre-launch cal/val of the GOES-R ABI (Nalli et al. 2008b). 53

8 Unenhanced digital color photograph of the forward 02 Level of the *Ronald H. Brown*, taken while holding station along 23°W longitude during PNE/AEROSE-III, the afternoon of 13 May 2007, during the major Saharan dust outflow pulse shown in Figure 7. Some AEROSE instrumentation visible in the foreground are, from left: broadband flux radiometers (i.e., pyranometers and pyrgeometers), all-sky camera, M-AERI, and microwave (MW) radiometer. 54

9 Skew-T Log-P diagrams of tropical Atlantic/Caribbean soundings: (Left) AEROSE-V (03:42 UTC 6 August 2009) sounding from western Atlantic (Caribbean Sea) just northeast of Puerto Rico (18.75°N, 65.12°W), (center) AEROSE-III (13:40 UTC 13 May 2007) sounding from the eastern Atlantic (9.50°N, 23.00°W) during major dust outflow (cf. Figures 7 and 8), and (right) Jul–Oct 2002 mean sounding (Caribbean Sea) for SAL conditions during the Atlantic hurricane season (Dunion and Marron 2008). The righthand y-axes show geopotential heights in kilometers for reference. Meteorological convention wind barbs designate metric wind speeds rounded to the nearest 2.5 $\mathrm{m\,s^{-1}}$and 5.0 $\mathrm{m\,s^{-1}}$for half and full feathers, respectively. 55


FIG. 1. NOAA Ship *Ronald H. Brown* tied up in San Juan, Puerto Rico, USA, just prior to departure for the first leg of the trans-Atlantic 2006 PNE/AEROSE-II cruise. Photo courtesy of A. Flores (Howard University).

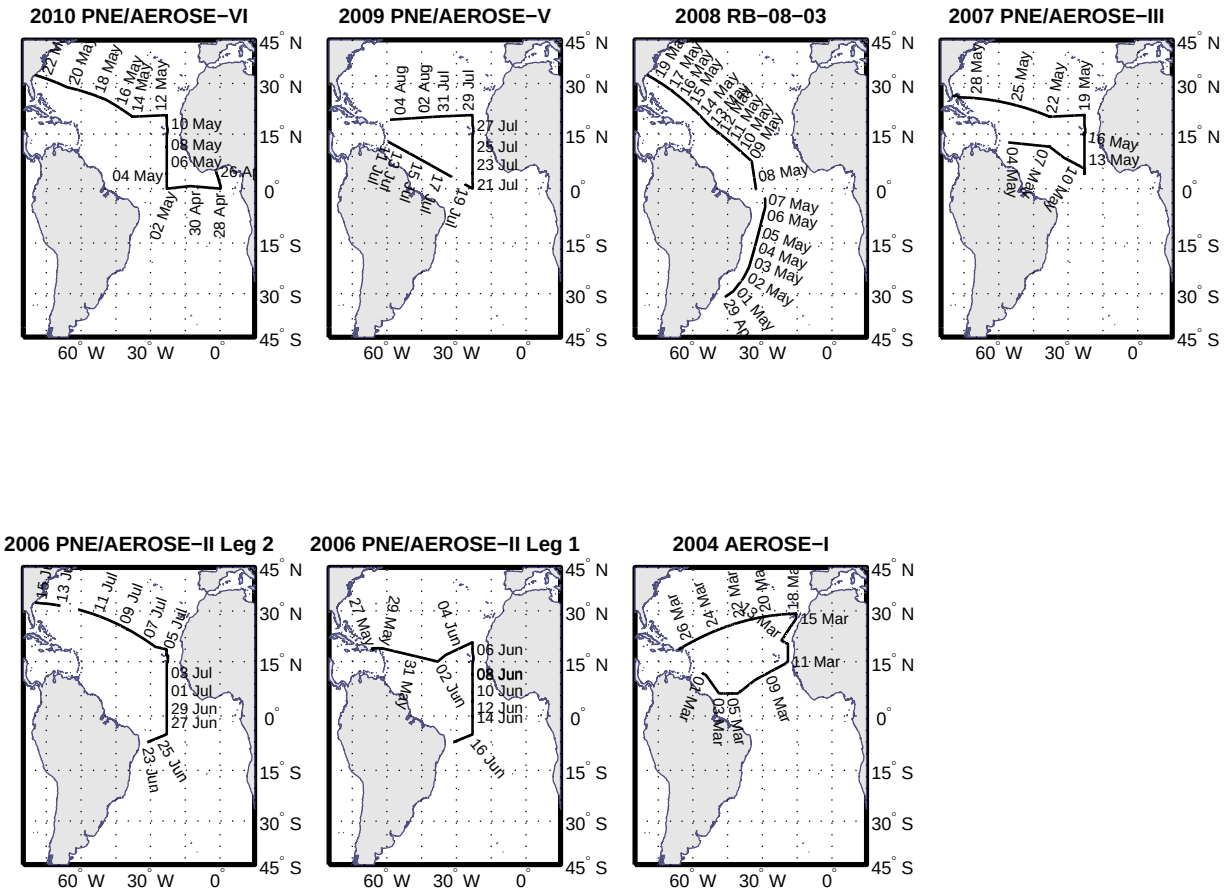


FIG. 2. AEROSE cruise tracks and dates. Areas of missing track lines are the result of data blackouts imposed on the *Ronald H. Brown* within Exclusive Economic Zones (EEZs) without prior clearance (e.g., Brazilian). Map projections are cylindrical equal-area.

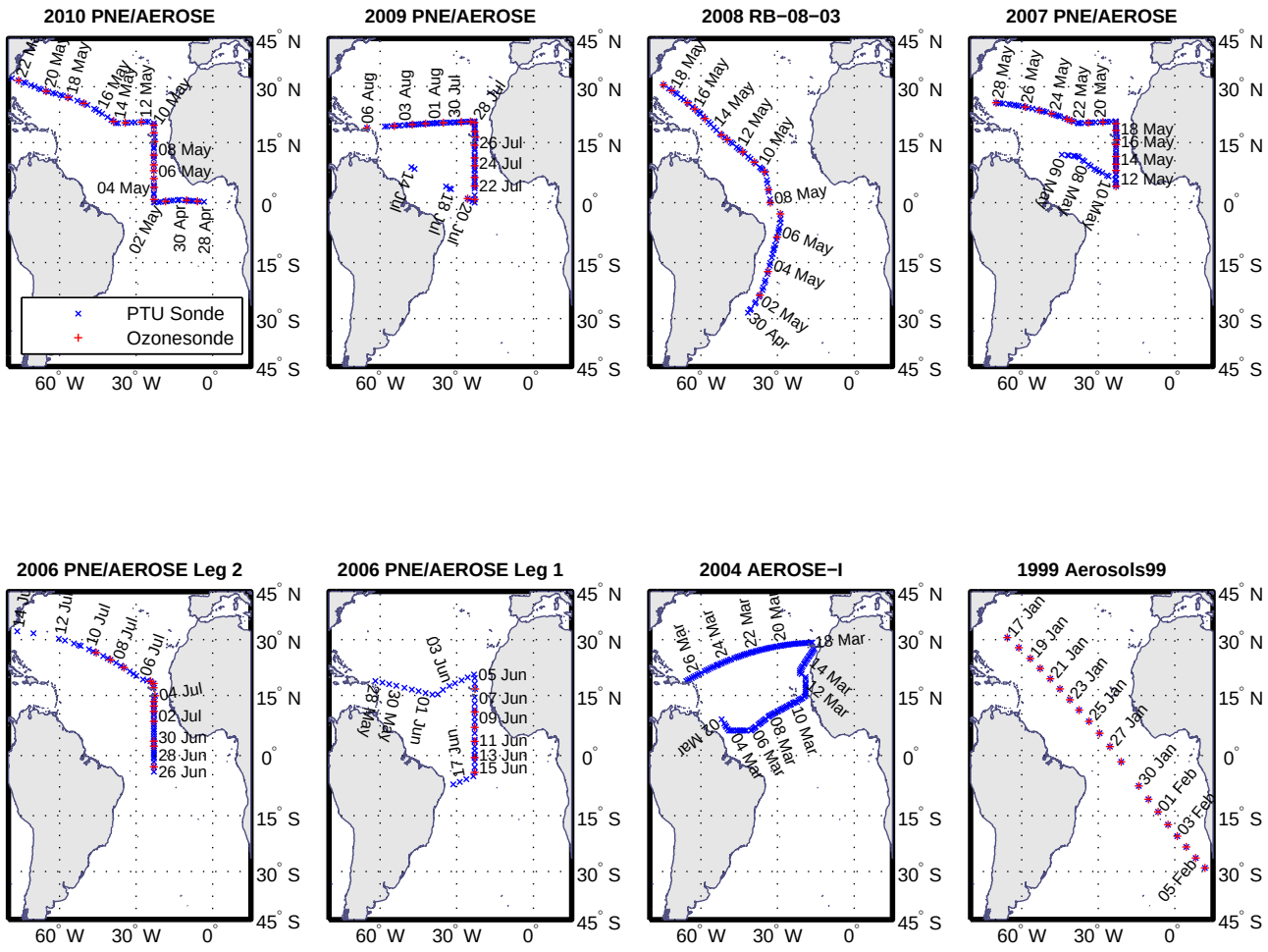


FIG. 3. Locations and dates of Vaisala PTU rawinsondes (blue ×) and ozonesondes (red +) launched during the AEROSE 2004, 2006–2010 campaigns. Locations of PTU/$O_3$ launches from the Aerosols99 cruise are also shown in the lower right plot for comparison. Map projections are cylindrical equal-area.

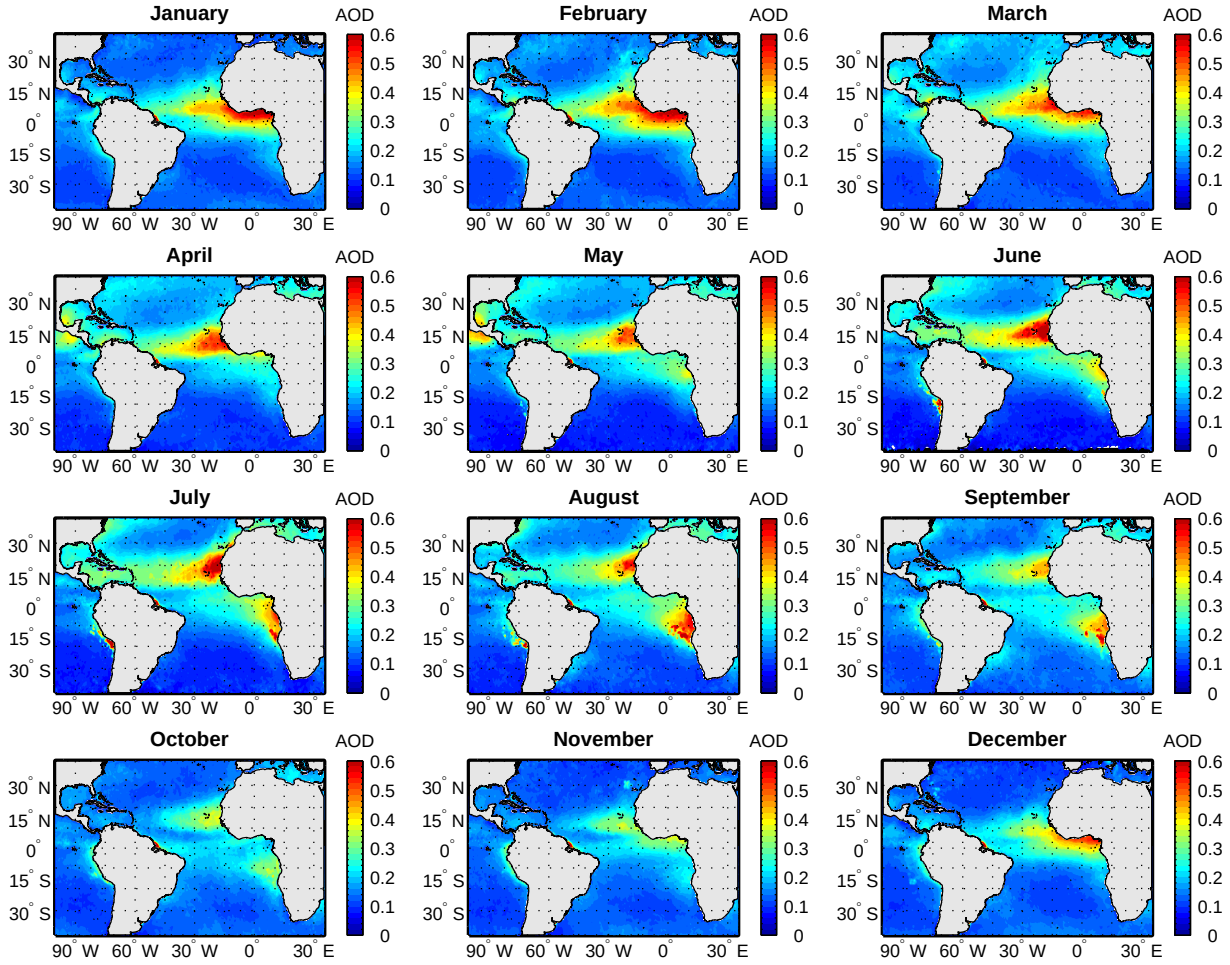


FIG. 4. AVHRR Pathfinder Atmospheres Extended (PATMOS-x) monthly climatological mean tropospheric aerosol optical depth (AOD) for a 1981–2008 base period, excluding years following volcanic eruptions, 1982–1984 and 1991–1993. The PATMOS-x AOD are derived from cloud-free AVHRR channel 1 ($\lambda = 0.63$ $\mu$m) normalized reflectances (cf., Jacobowitz et al. 2003; Zhao et al. 2008). Map projections are Mercator.

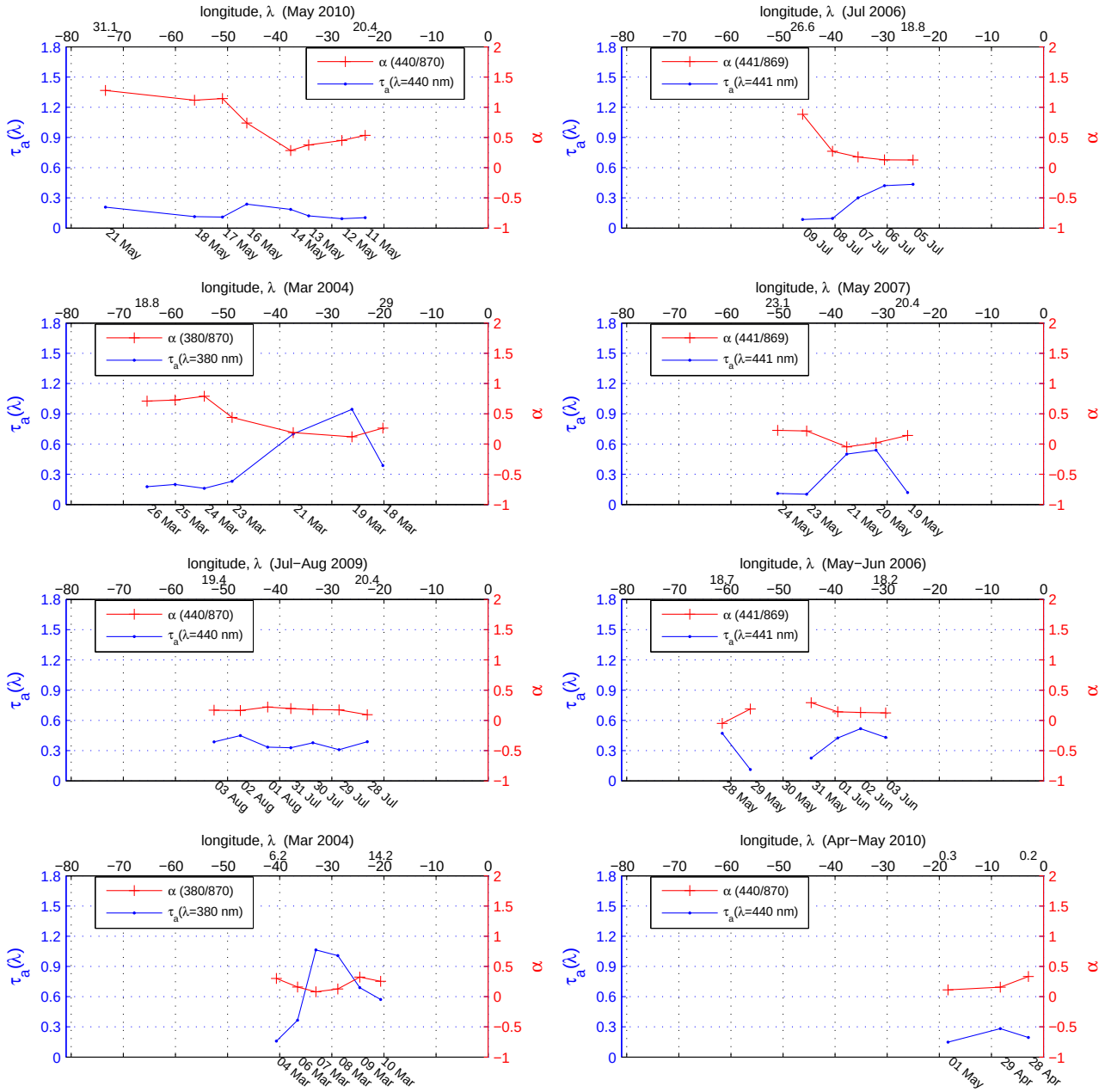


FIG. 5. Microtops sunphotometer daily mean AOD ($\tau_a$, blue) and derived Angstrom exponents ($\alpha$, red) for zonal AEROSE transects plotted on a common longitude scale. Small numbers above the main $x$-axis labeling denote the limits of the orthogonal axis (i.e., latitude). Raw AOD values have been processed according to the Maritime Aerosol Network (MAN) methodology (Smirnov et al. 2009). The plots are roughly "sorted" from left-to-right, top-to-bottom as north to south zonal sections.

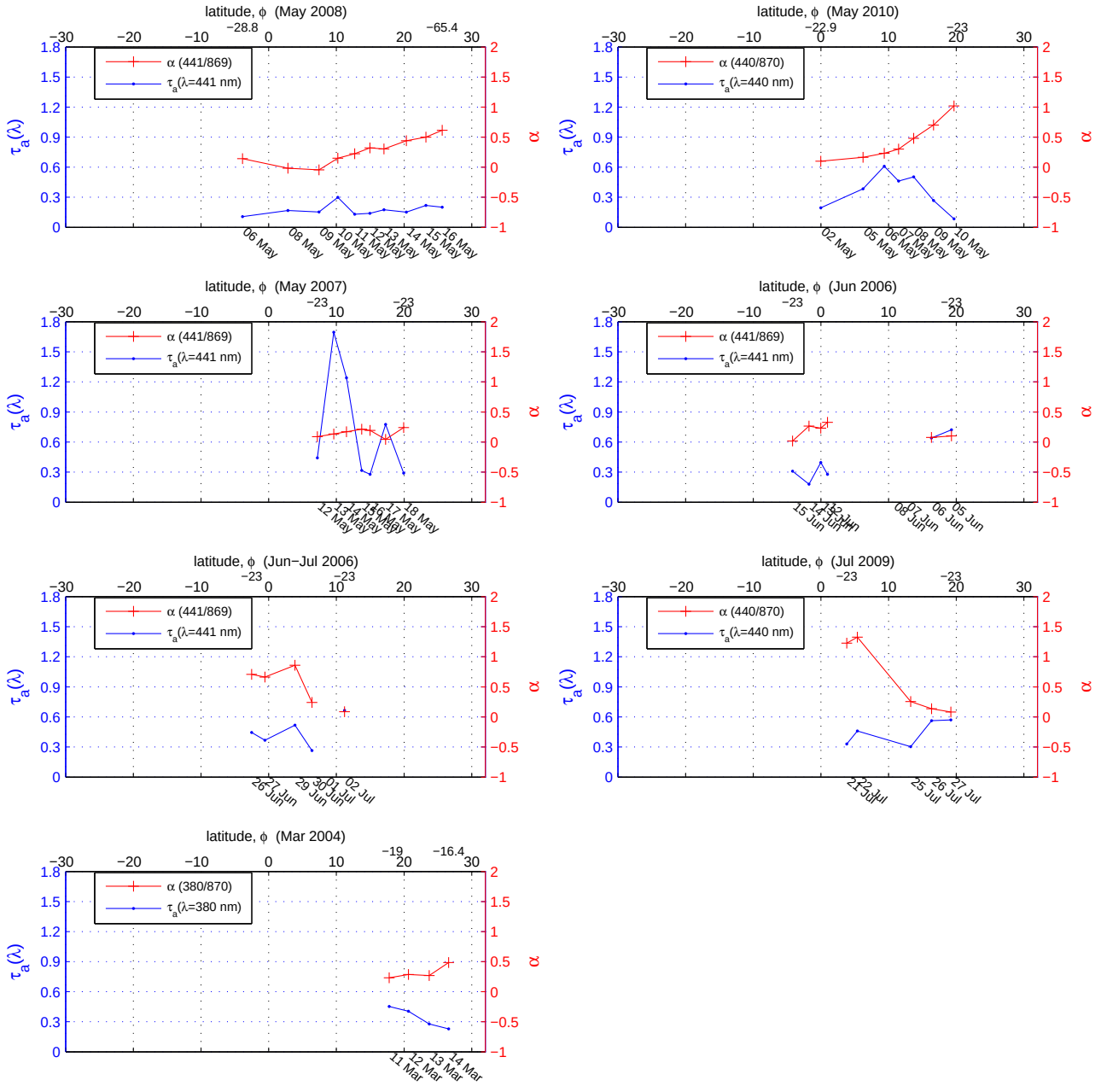


FIG. 6. As Figure 5 except for meridional AEROSE transects plotted on a common latitude scale. Small numbers above the main $x$-axis labeling denote the limits of the orthogonal axis (i.e., longitude). The plots are roughly "sorted" from left-to-right, top-to-bottom as first west to east meridional sections and then time of the year.

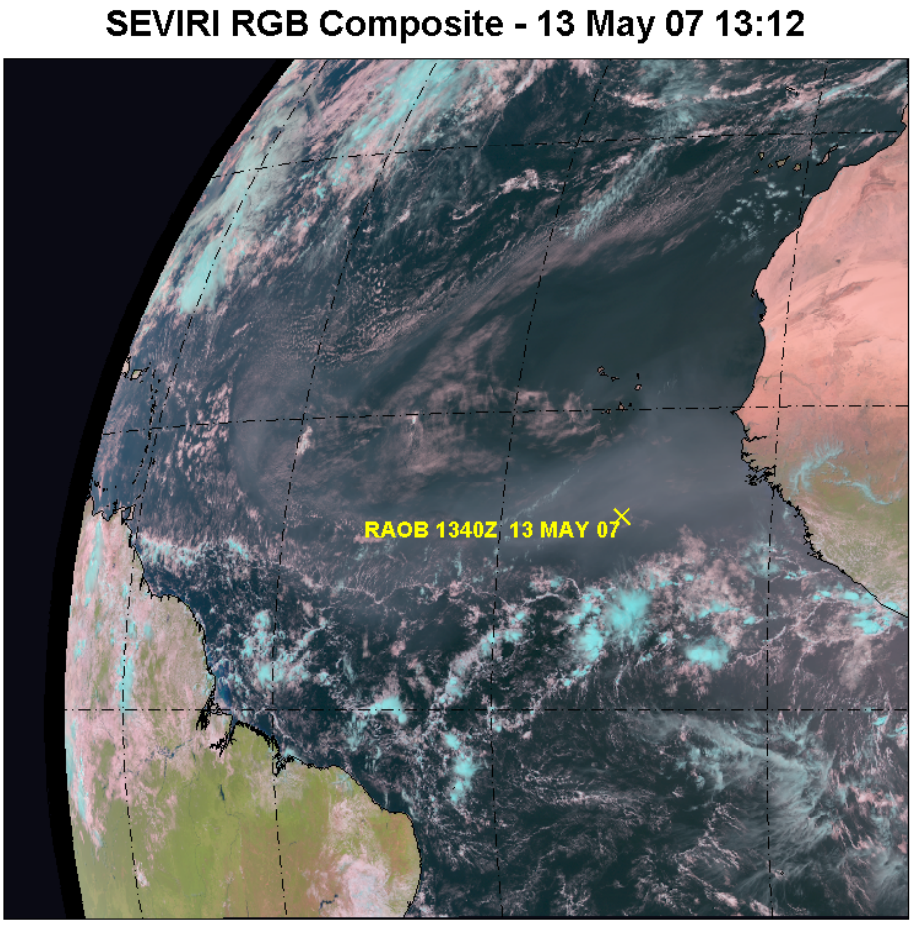


FIG. 7. SEVIRI RGB color-composite (using channels 1.6 $\mu$m, 0.8 $\mu$m and 0.6 $\mu$m for red, green and blue, respectively) 2-km imagery for the AEROSE domain, 13:12 UTC, 13 May 2007. The location of a coincident sonde launch (9.501°N, 22.998°W; 13:40 UTC) within a strong Saharan dust outflow plume (cf. Figure 9) is shown in yellow. Map projection is vertical perspective azimuthal. NESDIS/STAR has archived hourly 2-km SEVIRI multichannel data for all the AEROSE campaigns to create a marine-based GOES-R proxy dataset for pre-launch cal/val of the GOES-R ABI (Nalli et al. 2008b).

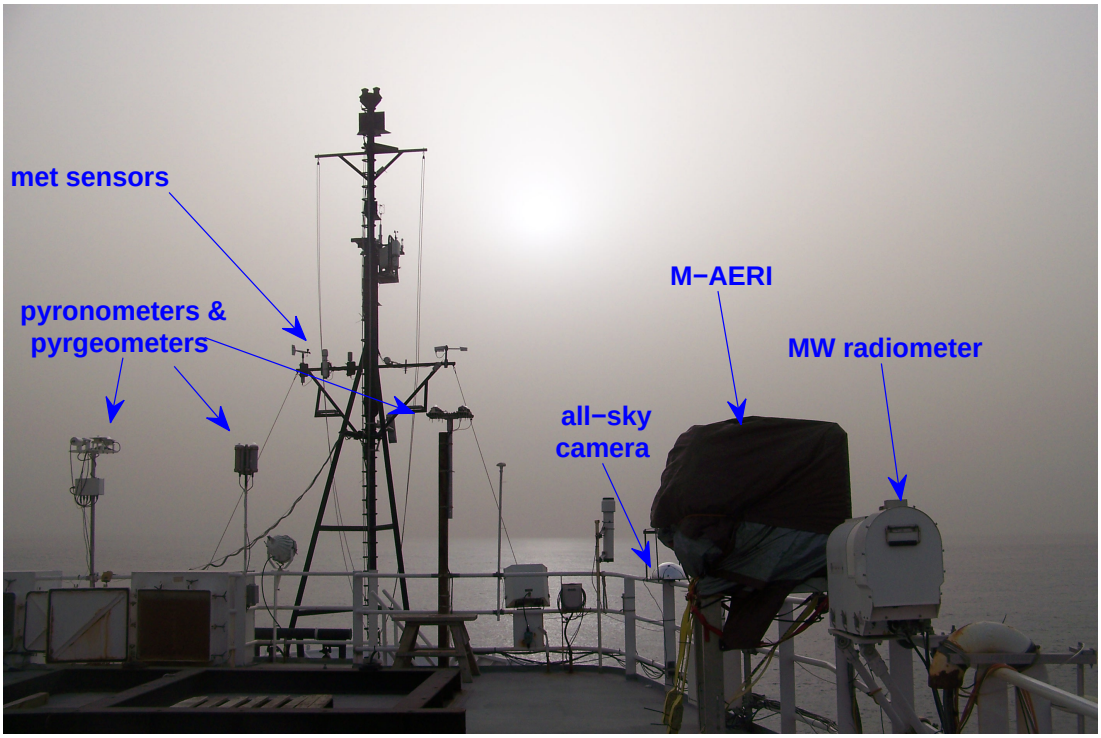


FIG. 8. Unenhanced digital color photograph of the forward 02 Level of the *Ronald H. Brown*, taken while holding station along 23°W longitude during PNE/AEROSE-III, the afternoon of 13 May 2007, during the major Saharan dust outflow pulse shown in Figure 7. Some AEROSE instrumentation visible in the foreground are, from left: broadband flux radiometers (i.e., pyranometers and pyrgeometers), all-sky camera, M-AERI, and microwave (MW) radiometer.

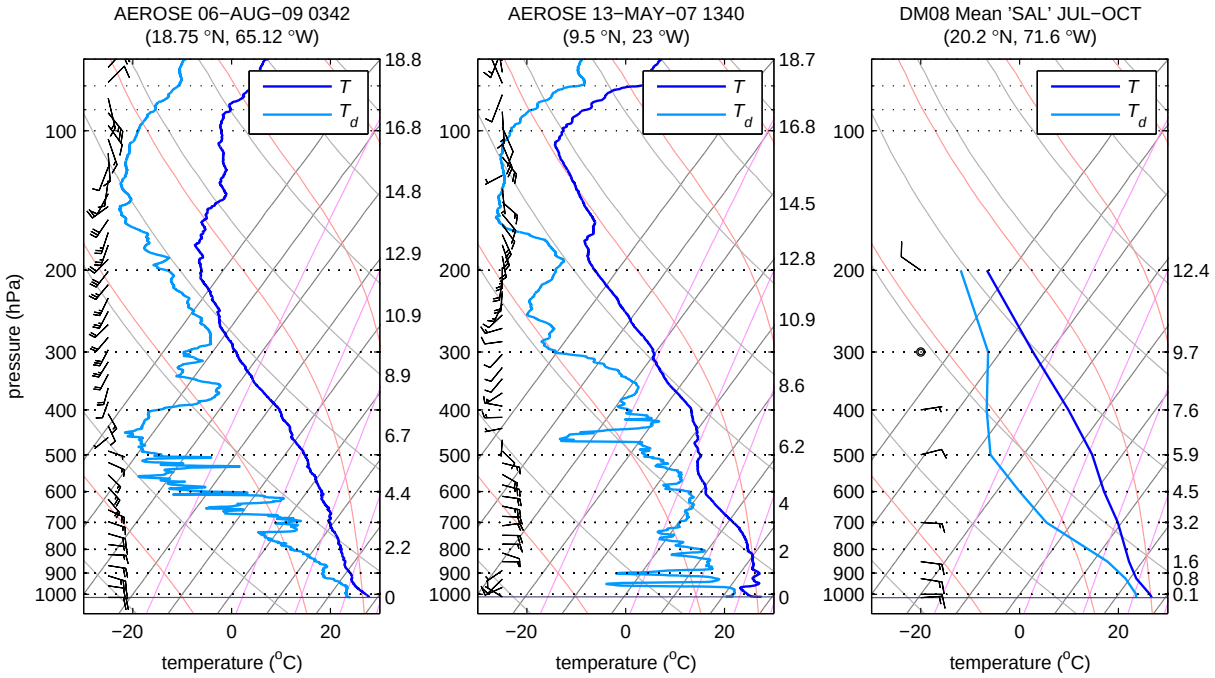


FIG. 9. Skew-T Log-P diagrams of tropical Atlantic/Caribbean soundings: (Left) AEROSE-V (03:42 UTC 6 August 2009) sounding from western Atlantic (Caribbean Sea) just northeast of Puerto Rico (18.75°N, 65.12°W), (center) AEROSE-III (13:40 UTC 13 May 2007) sounding from the eastern Atlantic (9.50°N, 23.00°W) during major dust outflow (cf. Figures 7 and 8), and (right) Jul–Oct 2002 mean sounding (Caribbean Sea) for SAL conditions during the Atlantic hurricane season (Dunion and Marron 2008). The righthand y-axes show geopotential heights in kilometers for reference. Meteorological convention wind barbs designate metric wind speeds rounded to the nearest 2.5 $\mathrm{m\,s^{-1}}$and 5.0 $\mathrm{m\,s^{-1}}$for half and full feathers, respectively.

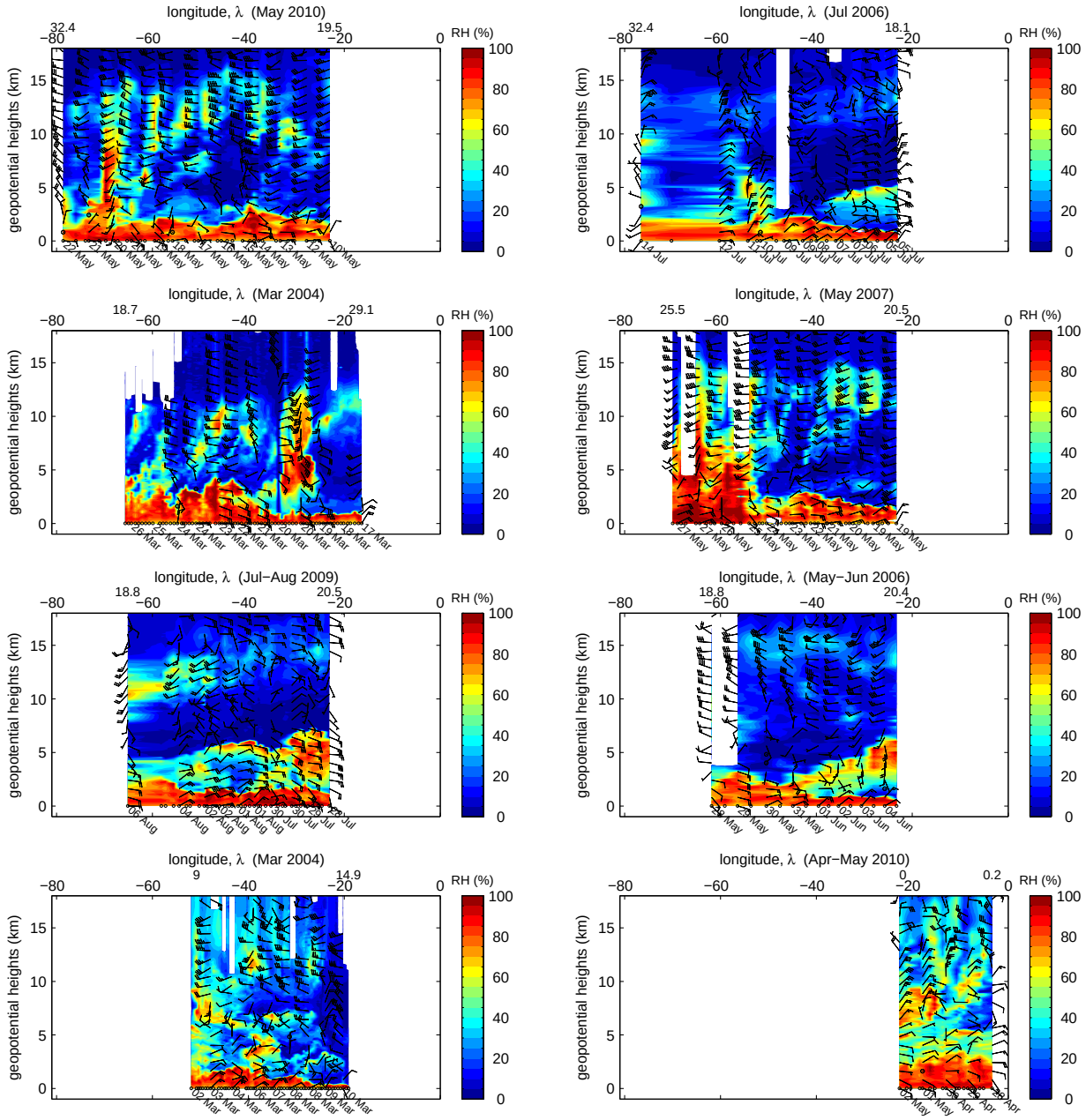


FIG. 10. Zonal cross-sectional contour analyses of Vaisala radiosonde RH measurements (%), expressed as a function of longitude and geopotential heights, $z_g$ (km), obtained during the AEROSE campaigns. Small numbers above the main $x$-axis labeling denote the limits of the orthogonal axis (i.e., latitude). Horizontal-component wind vector measurements are overlaid (for clarity, only a subsample of wind vectors is shown); speeds are expressed in SI units using half, full and pennant feathers for increments of 2.5, 5.0, and 25 $\mathrm{m\,s^{-1}}$, respectively. Sonde launch locations are shown by gray circles at the surface; dates are shown for the wind vector subsamples. Longitude scales and transect subplot-ordering are as in Fig. 5.

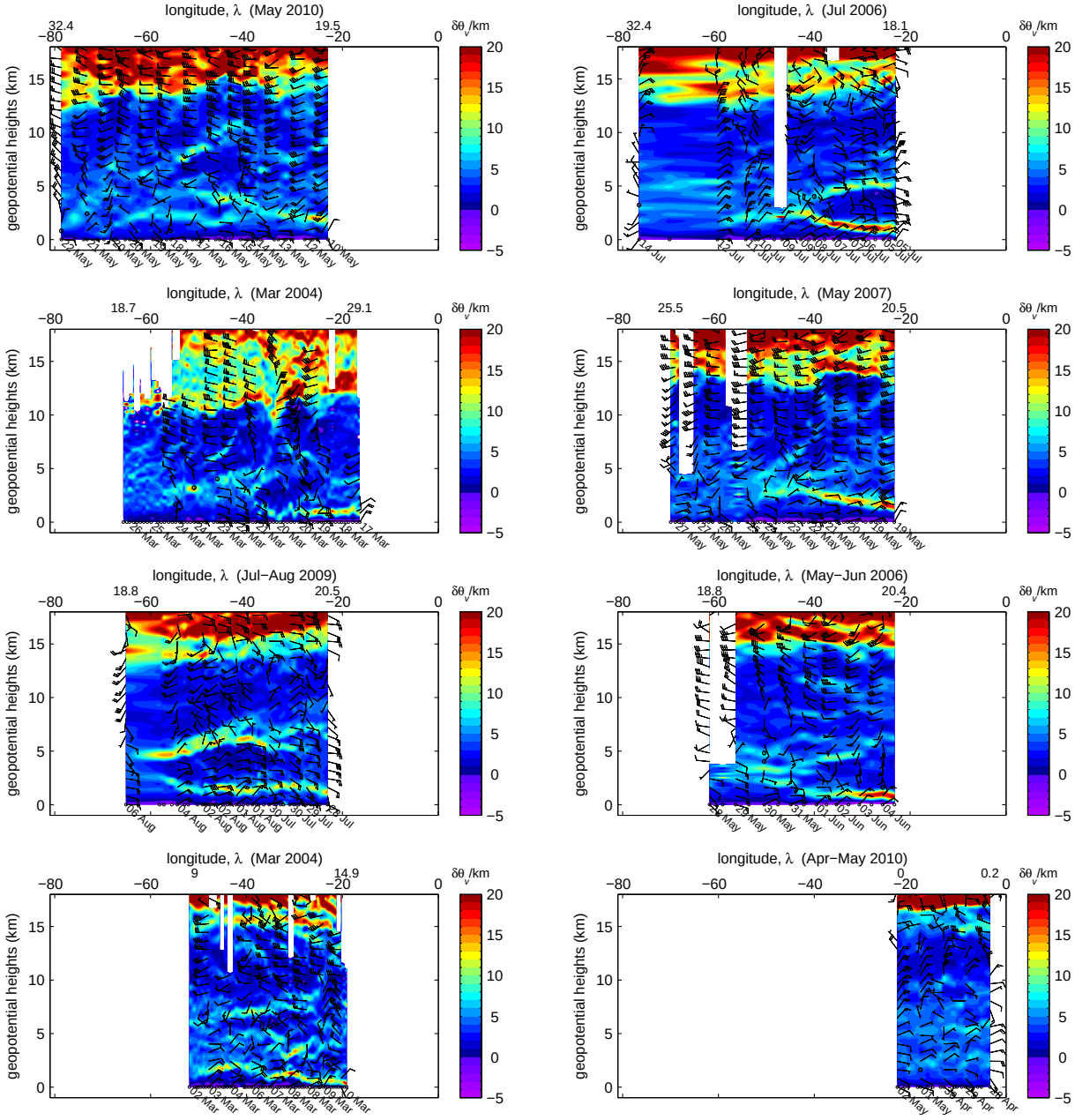


FIG. 11. As Figure 10 except for virtual potential temperature lapse rate (VPTLR), $\delta\theta_v/\delta z$.

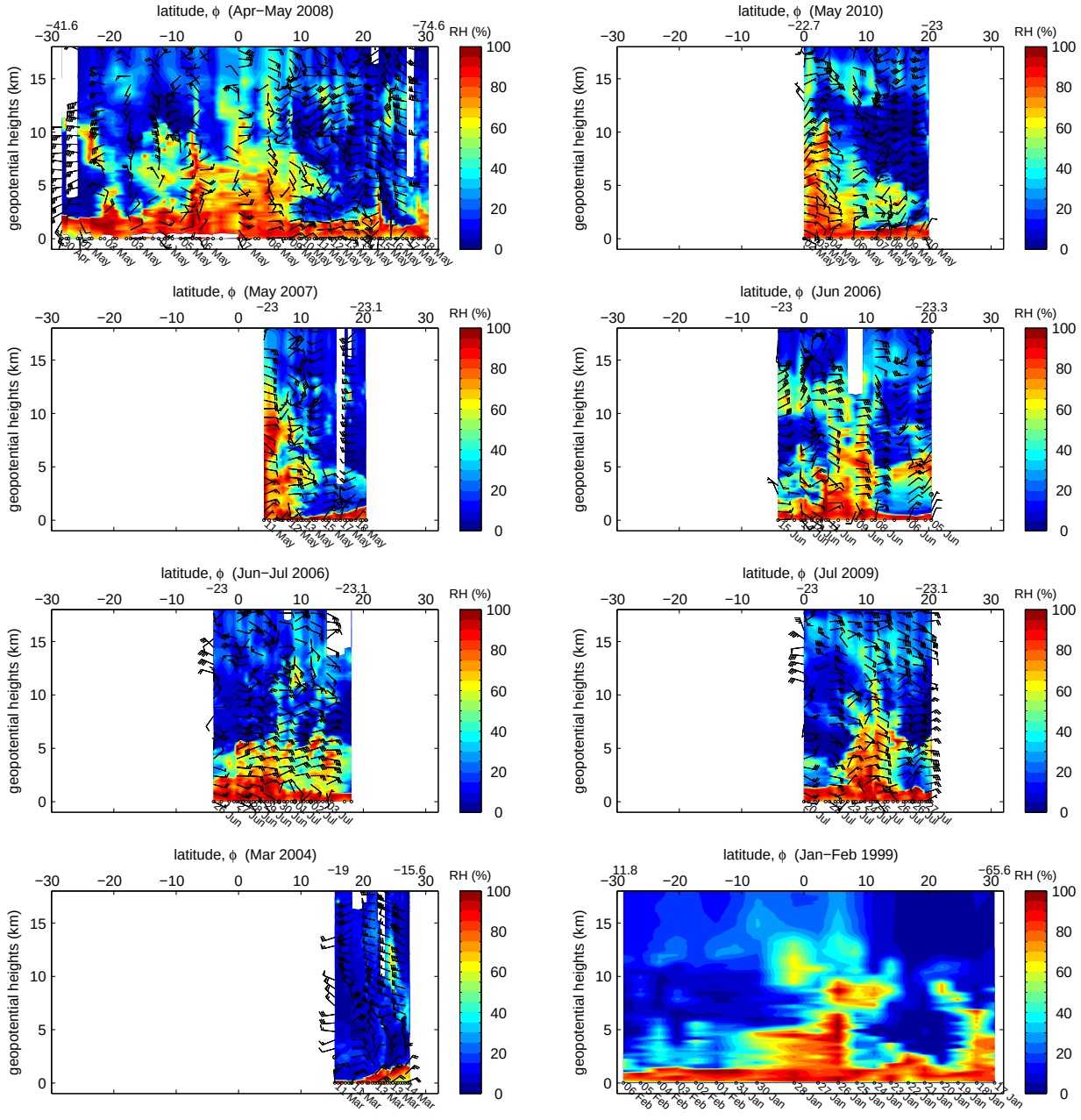


FIG. 12. As Figure 10 except meridional cross-sections, with small numbers above the main $x$-axis labeling denoting the limits of the orthogonal axis (i.e., longitude). The lower right panel shows results from sondes launched during the Aerosols99 cruise (cf., Bates et al. 2001) for comparison. Latitude scales and transect subplot-ordering are as in Fig. 6.

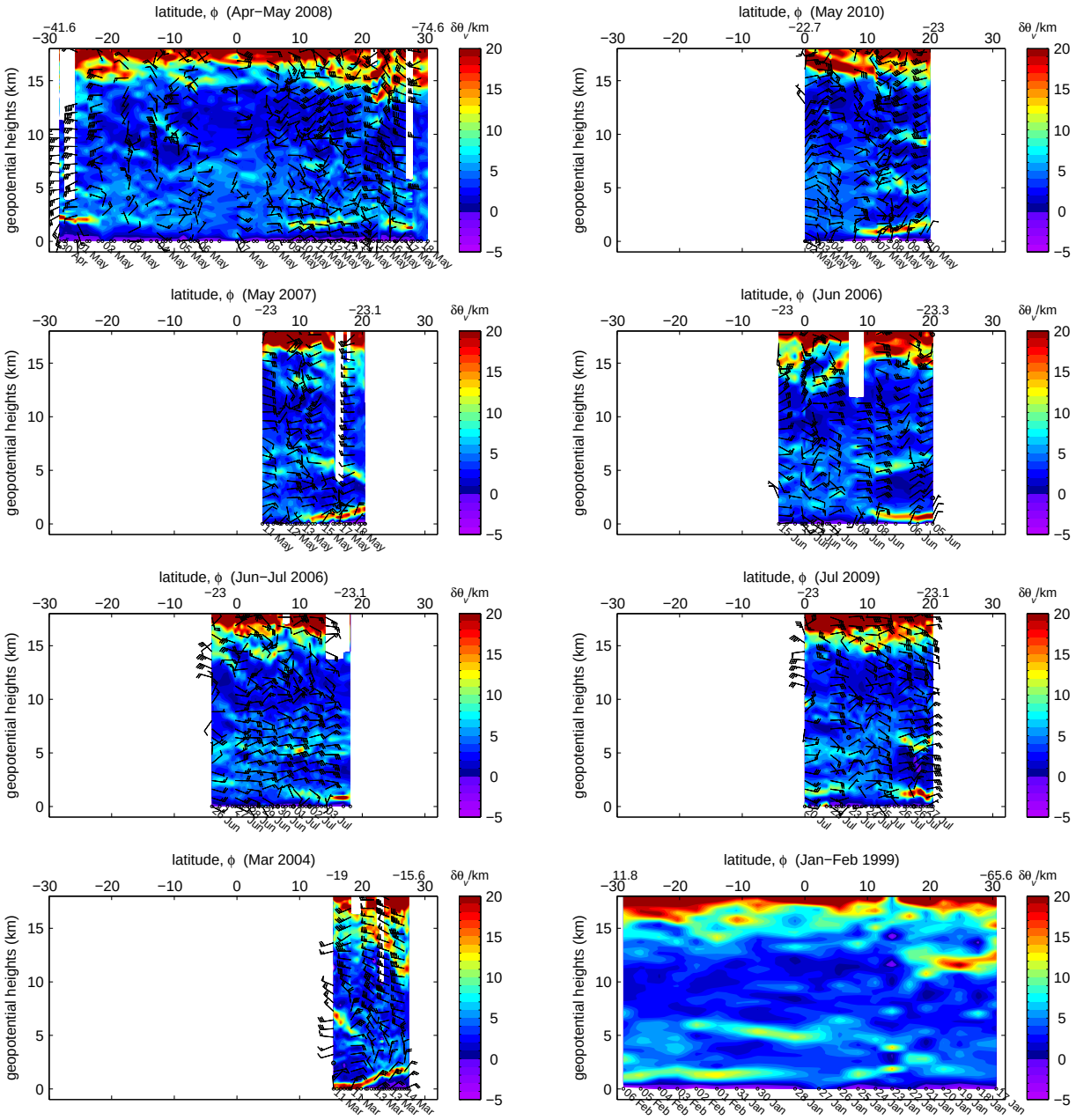


FIG. 13. As Figure 12 except except VPTLR, $\delta\theta_v/\delta z$.

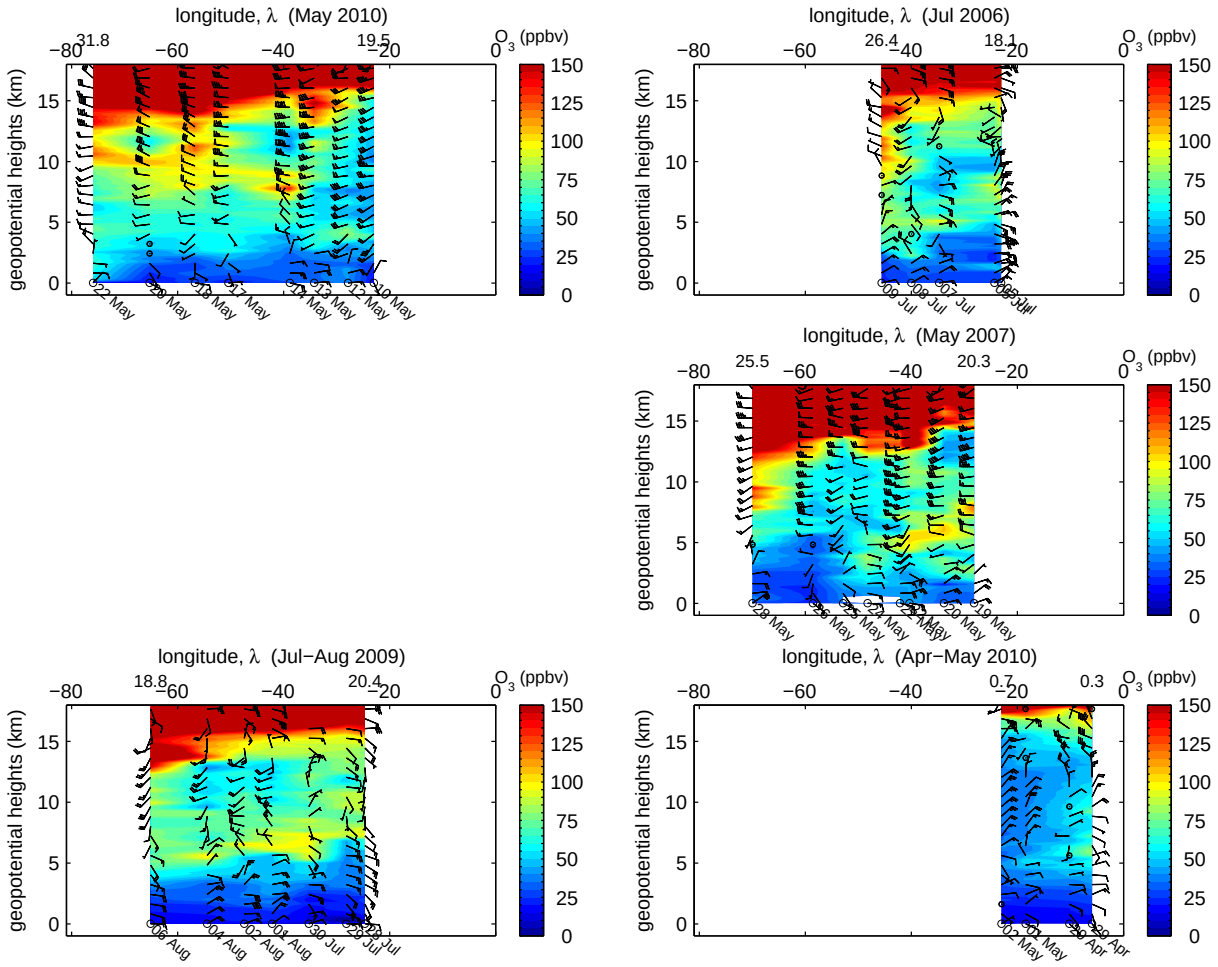


FIG. 14. As Figures 10 and 11 except zonal cross-sectional contour analyses of ozonesonde $O_3$ measurements, with partial pressure converted to volumetric mixing ratio in PPBV using the concurrent RS92 PTU measurements.

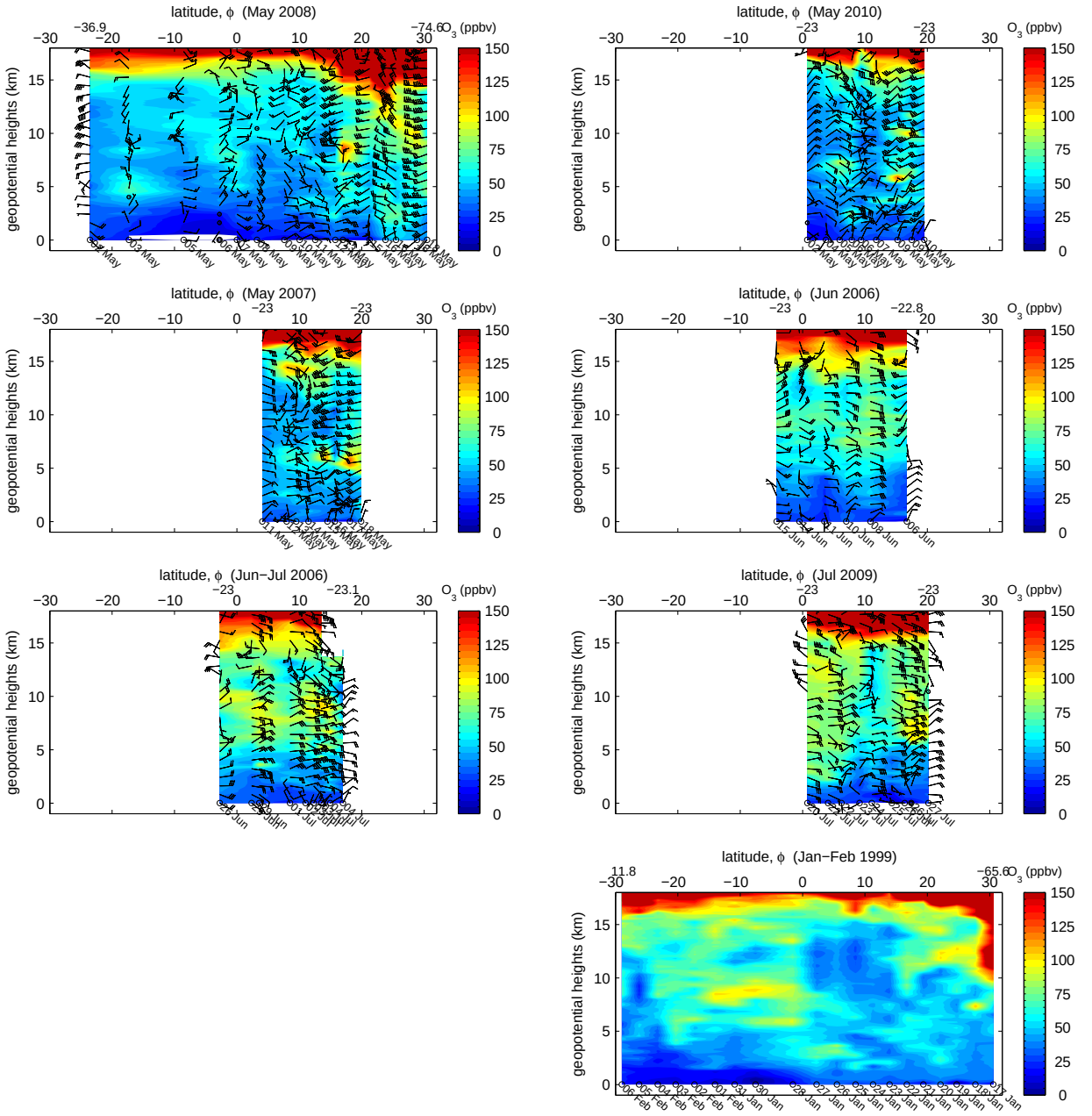


FIG. 15. As Figure 14 except zonal cross sections, the lower right panel showing results from ozonesondes launched during the Aerosols99 cruise for comparison (cf. Thompson et al. 2000).

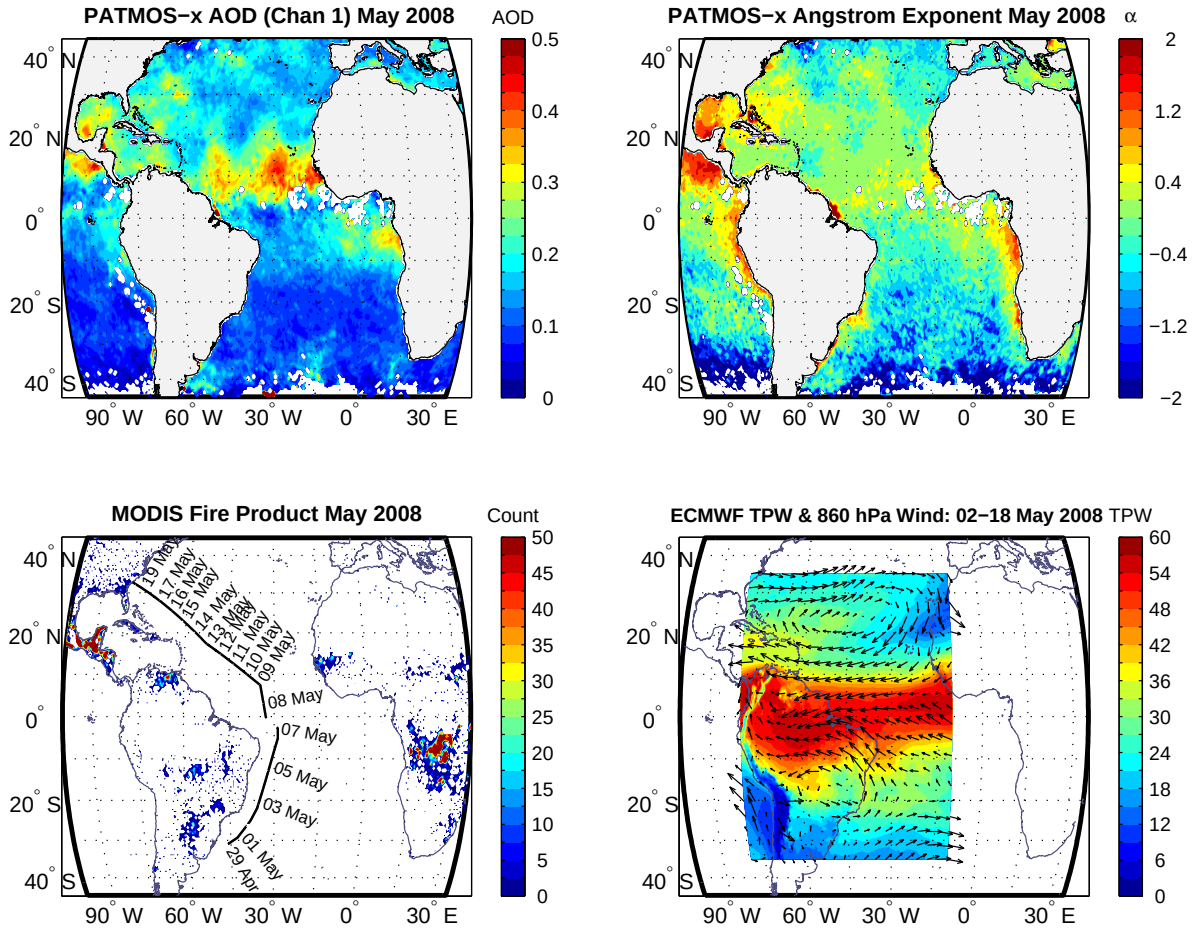


FIG. 16. Prevailing aerosol, fire, wind and water vapor conditions during the RB-08-03 interhemispheric transit (May 2008): (top left) PATMOS-x AVHRR mean channel 1 (0.63 $\mu$m) AOD, (top right) mean Angstrom exponent ($\alpha$) derived from channels 1 and 2 (0.63, 0.83 $\mu$m), (lower left) total fire counts from the MODIS CMG Fire Product (Giglio et al. 2003) (with RB-08-03 cruise track superimposed), and (lower right) mean 860 hPa wind and TPW fields from the ECMWF model analysis (restricted to the AEROSE space-time domain, 2-18 May). Map projections are equal-area.